19th International Workshop on Optical Waveguide Theory and Numerical Modelling

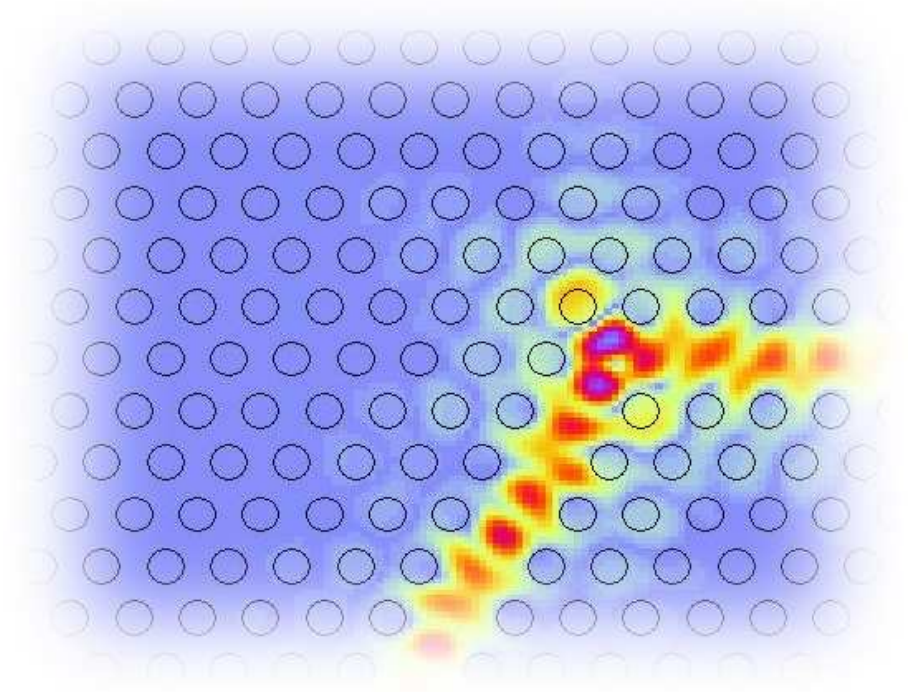

20th – 21st April 2012

Barcelona, Spain

Hosted by:

The Institute of Photonic Sciences (ICFO), Barcelona

The George Green Institute for Electromagnetics Research
University of Nottingham

Optical Waveguide Theory and Numerical Modelling Workshop 2012
Workshop Programme

		Thursday 19th April
		Registration: Open all days of the ECIO+OWTNM Meeting
		Friday 20th April
08:30 – 09:15		**Plenary: PIC's: A Commercial Future** Mike Wale - Oclaro Technology Limited, UK
09:25 – 09:30		**Opening remarks, Professor Trevor M Benson, University of Nottingham, UK** **Location: Tramuntana 1**
Session 1 **09:30 - 10:45**	**FrA**	**Plasmonics** **Chair: Professor Trevor M. Benson, University of Nottingham, UK** **Location: Tramuntana 1**
09:30 - 10:00	FrA1	**Plasmonic Waveguides in the Optical and Terahertz Regimes (Invited)** *F. J. Garcia-Vidal*
10:00 - 10:20	FrA2	**The Wire Grid as a Plasmonic Reflective Polarizer** *H. S. Tonchev, O. Parriaux*
10:20 - 10:40	FrA3	**Numerical Solution of Nonlocal Hydrodynamic Drude Model for Arbitrary Shaped Nano-plasmonic Structures using Nédélec Finite Elements** *K. R. Hiremath, L. Zschiedrich, S. Burger, F. Schmidt*
10:45 - 11:15		**Coffee Break , Location: Hall of the Auditorium**
Session 2 **11:15 – 12:35**	**FrB**	**Methods and Applications I ; Location: Tramuntana 1** **Chair: Dr G Morozov, University of the West of Scotland, UK**
11:15 - 11:35	FrB1	**Angularly Robust Resonant Reflection by Grating-induced Mode Coalescence** *A. V. Tishchenko and O. Parriaux*
11:35 - 11:55	FrB2	**Modeling Reflections Induced by Waveguide Transitions** *D. Melati, F. Morichetti, A. Meloni*
11:55 - 12:15	FrB3	**Tailored Design for WDM Filters in BCB-embedded PhC Membranes** *S. Malaguti, G. Bellanca, S. Trillo*
12:15 - 12:35	FrB4	**Local Boundary Condition for Terminating Photonic Crystal Waveguides** *Z. Hu, Y. Y. Lu*

12:45 - 13:45		**Lunch Break, Location: Hall of the Auditorium**
Session 3 **13:45 - 15:00**	**FrJC**	**Joint Session with ECIO: Design and Modelling** **Chair: Dominic Gallagher, Photon Design.**
13:45 - 14:15	FrJC1	**Optical Waveguide Engineering for Demanding Applications (ECIO Invited)** *I. Molina-Fernández*
14:15 - 14:30	FrJC2	**Fourier Series based 3D Bi-directional Propagation for Integrated Photonics** *J. Čtyroký, P. Kwiecien, I. Richter*
14:30 – 14:45	FrJC3	**Analytical Approach towards Fishnet Negative Index of Refraction** *J. Fiala, P, Kwiecien, I. Richter*
14:45 - 15:00	FrJC4	**Simulation of Optical Forces on a Microparticle on an Optical Waveguide** *O. G. Hellesø, P. Løvhaugen*
15:00 – 15:30		**Coffee available in Hall of the Auditorium**
Session 4 **15:00 – 16:00**		**Poster Presentations, Location: Hall of the Auditorium**
	P1	**FDTD Simulation of Acousto-optic Filter with Beam Expanders Constituted by Photonic Crystal Rows of Airholes in LiNbO3 Waveguides** *A. V. Tsarev*
	P2	**Compact Multi-splitting Widely Tunable Filter on SOI Technology** *A. V. Tsarev*
	P3	**Large Integrated Spot Size Converter for an InGaAs Pin-photodiode** *A. Wieczorek, Y. Hua, B. Roycroft, F. H. Peters, B. Corbett*
	P4	**A Factorable Photon Pair Source based on Silicon Nanowires** *S. Khasminskaya, H. X. Tang, W. H. P. Pernice*
	P5	**Three-dimensional FFT-based Generalized Rectangular Wide-angle Beam Propagation Method with Complex Jacobi Iteration** *R. Godoy-Rubio, A. Ortega-Moñux*
	P6	**Nonlinear Surface Wave Peculiarities in the Metal Covered SBN:75 Photorefractive Crystal** *J. Nurligareev, B. Usievich, V. Sychugov, L. Ivleva*
	P7	**Transformation of Whispering Gallery Waves in a Spherical Resonator caused by Permittivity Time Changing** *N. Sakhnenko, A. Nerukh, T. Remayeva, T. Benson*
	P8	**Waveguide Laser Modelling of Erbium/Ytterbium Activated Monoclinic Double Tungstates** *J. Martínez de Mendibil, G. Lifante, C. Berrospe, W. Bolaños, J. J. Carvajal, M. Aguiló, F. Días, E. Cantelar*

	P9	**Impact of Hosting Media on the Specific Resonances of Periodic Grating Embedded in Dielectric Slab** *V. Byelobrov, T. Benson, A. Nosich*
	P10	**Analysis of 2D Photonic Bandgap Waveguides using a Simple Analytical Method** *K. Gehlot, A. Sharma*
Session 5 **16:00 - 17:00**	**FrD**	**Methods and Applications II** **Chair: Olivier Parriaux, University of Lyon at Saint-Etienne, France** **Location: Tramuntana 1**
16:00 - 16:20	FrD1	**Modelling of Nanoparticle Arrays in Si Solar Cells** *R, Carius, D. Michaelis, E. Moulin, U. Paetzold, C. Wächter*
16:200 - 16:40	FrD2	**Fast Thermo-optic Wavelength Scanning for Sensors Interrogation in SOI Technology** *A. V. Tsarev, F. De Leonardis, V. M. N. Passaro*
16:40 - 17:00		**Open Forum and Preliminary Post-Deadline results**
17:00		**Workshop Photo**
		Saturday 21st April
Session 6 **09:25 – 10:45**	**SaA**	**Photonic Crystals** **Chair: Christoph Waechter, Fraunhofer Institut fuer Angewandte Optik und Feinmechanik, Jena** **Location: Tramuntana 1**
09:25 - 09:45	SaA1	**A Multiscale FEM for 2D Photonic Crystal Bands** *H. Brandsmeier, K. Schmidt, C. Schwab*
09:45 - 10:05	SaA2	**Floquet-Bloch Waves for TM-polarized Light in 1D Photonic Crystals** *G. V. Morozov, D. W. L. Sprung*
10:05 – 10:25	SaA3	**Efficient Boundary Integral Equation Method for Photonic Crystal Fibers** *W. Lu, Y. Y. Lu*
10:25 - 10:45	SaA4	**Mode Field Diameter of Index Guided Photonic Crystal Fibers** *D. K. Sharma, A. Sharma*
10:45 - 11:15		**Coffee Break, Location: Hall of Tramuntana 1**
Session 7 **11:15 - 12:55**	**SaB**	**Methods and Application III** **Chair: Manfred Hammer, University of Twente** **Location: Tramuntana 1**

11:15 - 11:35	SaB1	**Finite Element Analysis of Anisotropic Optical Waveguides with Arbitrary Optic-Axis Orientation** *H-H. Liu, H-C. Chang*
11:35 - 11:55	SaB2	**Waveguiding Properties of Ribbed Surface Waveguides in Three Frequency Domains** *C. A. Jones, S. F. Helfert, J. Jahns*
11:55 - 12:15	SaB3	**Simulation of Reflection in Volume Bragg Grating and Tilted Fiber Bragg Grating Structures using a Bidirectional Split-step Finite Difference Method** *D. Bhattacharya, A. Sharma*
12:15 - 12:35	SaB4	**Efficient Analysis of Bent Waveguides with Fourier Modal Methods** *L. Zavargo-Peche, J. Čtyroký, A. Ortega-Moñux, J. Gonzalo Wangüemert-Pérez, I. Molina-Fernández*
12:35 - 12:55	SaB5	**3D Photonic Structure Modeling with Efficient Fourier Modal Methods** *P. Kwiecien, I. Richter, J. Čtyroký*
13:00 - 13:45		**Lunch Break, Location: Hall of Tramuntana 1**
Session 8 **13:45 - 15:25**	**SaC**	**Methods and Applications IV** **Chair: J. Čtyroký, Institute of Photonics and Electronics Prague** Location:
13:45 - 14:05	SaC1	**Simulation of 3D Photonic Nanostructures using a Bidirectional Eigenmode Propagation Algorithm** *J. Luksch, J. Petráček*
14:05 - 14:25	SaC2	**Novel Silicon Wire Waveguide Crossing with Negligible Loss and Crosstalk** *A. V. Tsarev*
14:25 - 14:45	SaC3	**A New TLM Model for Thin Optical Features** *X. Meng, P. Sewell, A. Vukovic, T. M. Benson*
14:45 – 15:05	SaC4	**Propagation of a Gaussian Pulse in a Coaxial Optical Fiber: Effect of Two Mode Interference** *E. K. Sharma, J. Anand, J. K. Anand*
15:05 - 15:25	SaC5	**HCMT Interaction of Whispering Gallery Modes in Circuits of Integrated Optical Microring or -Disk Resonators** *E. F. Franchimon, K. R. Hiremath, R. Stoffer, M. Hammer*
15:25		**Concluding Remarks, announcement of Special Issue of Optical and Quantum Electronics, and the Next OWTNM**
15:30		**CLOSE**

OWTNM 2012 CONTENTS

PAPERS

A Multiscale FEM for 2D Photonic Crystal Bands
H. Brandsmeier, K. Schmidt, C. Schwab

Floquet-Bloch Waves for TM-polarized Light in 1D Photonic Crystals
G. V. Morozov, D. W. L. Sprung

Efficient Boundary Integral Equation Method for Photonic Crystal Fibers
W. Lu, Y. Y. Lu

Mode Field Diameter of Index Guided Photonic Crystal Fibers
D. K. Sharma, A. Sharma

Finite Element Analysis of Anisotropic Optical Waveguides with Arbitrary Optic-Axis Orientation
H-H. Liu, H-C. Chang

Waveguiding Properties of Ribbed Surface Waveguides in Three Frequency Domains
C. A. Jones, S. F. Helfert, J. Jahns

Simulation of Reflection in Volume Bragg Grating and Tilted Fiber Bragg Grating Structures using a Bidirectional Split-step Finite Difference Method
D. Bhattacharya, A. Sharma

Efficient Analysis of Bent Waveguides with Fourier Modal Methods
L. Zavargo-Peche, J. Čtyroký, A. Ortega-Moñux, J. Gonzalo Wangüemert-Pérez, I. Molina-Fernández

3D Photonic Structure Modeling with Efficient Fourier Modal Methods
P. Kwiecien, I. Richter, J. Čtyroký

Simulation of 3D Photonic Nanostructures using a Bidirectional Eigenmode Propagation Algorithm
J. Luksch, J. Petráček

Novel Silicon Wire Waveguide Crossing with Negligible Loss and Crosstalk
A. V. Tsarev

A New TLM Model for Thin Optical Features
X. Meng, P. Sewell, A. Vukovic, T. M. Benson

Propagation of a Gaussian Pulse in a Coaxial Optical Fiber: Effect of Two Mode Interference
E. K. Sharma, J. Anand, J. K. Anand

HCMT Interaction of Whispering Gallery Modes in Circuits of Integrated Optical Microring or -Disk Resonators
E. F. Franchimon, K. R. Hiremath, R. Stoffer, M. Hammer

POSTERS

FDTD Simulation of Acousto-optic Filter with Beam Expanders Constituted by Photonic Crystal Rows of Airholes in LiNbO3 Waveguides
A. V. Tsarev

Compact Multi-splitting Widely Tunable Filter on SOI Technology
A. V. Tsarev

Large Integrated Spot Size Converter for an InGaAs Pin-photodiode
A. Wieczorek, Y. Hua, B. Roycroft, F. H. Peters, B. Corbett

A Factorable Photon Pair Source based on Silicon Nanowires
S. Khasminskaya, H. X. Tang, W. H. P. Pernice

Three-dimensional FFT-based Generalized Rectangular Wide-angle Beam Propagation Method with Complex Jacobi Iteration
R. Godoy-Rubio, A. Ortega-Moñux

Nonlinear Surface Wave Peculiarities in the Metal Covered SBN:75 Photorefractive Crystal
J. Nurligareev, B. Usievich, V. Sychugov, L. Ivleva

Transformation of Whispering Gallery Waves in a Spherical Resonator caused by Permittivity Time Changing
N. Sakhnenko, A. Nerukh, T. Remayeva, T. Benson

Waveguide Laser Modelling of Erbium/Ytterbium Activated Monoclinic Double Tungstates
J. Martínez de Mendibil, G. Lifante, C. Berrospe, W. Bolaños, J. J. Carvajal, M. Aguiló, F. Días, E. Cantelar

Impact of Hosting Media on the Specific Resonances of Periodic Grating Embedded in Dielectric Slab
V. Byelobrov, T. Benson, A. Nosich

Analysis of 2D Photonic Bandgap Waveguides using a Simple Analytical Method
K. Gehlot, A. Sharma

Plasmonic waveguides in the optical and terahertz regimes

Francisco J. Garcia-Vidal
[1] *Departamento de Fisica Teorica de la Materia Condensada, Universidad Autonoma de Madrid, Madrid 28049 (Spain)*
fj.garcia@uam.es

In the first part of the talk, we will review recent developments in the search for building-up a kind of nanophotonic circuitry in the optical regime based on the capabilities of surface plasmon polaritons. We will put more emphasis on two routes that look very promising. 1) The so-called channel plasmons (CPs) that run in V-grooves perforated on metallic films.. We will describe in detail the propagation characteristics of these surface waves and how these properties can be tailored by just tuning the geometry of the groove [1]. 2) An alternative way for light routing uses the surface plasmons that propagate along metallic wedges, termed as wedge plasmons (WPs). We will show how these WPs present similar propagation lengths to those of CPs but they present a more pronounced subwavelength confinement [2].

In the second part of the presentation we will show how all the capabilities of surface plasmons found in the optical range of the electromagnetic spectrum can be safely transferred to lower frequencies (for example, terahertz frequencies) by taking advantage of the concept of *spoof* surface plasmon, i.e., surface electromagnetic modes in a nearly perfect electric conductor can be built up by periodically structuring its surface in a length scale much smaller than the operating wavelength. In particular, we will present three different strategies that take advantage of that concept to construct plasmonic waveguides in the terahertz regime: i) what we call spoof channel plasmons [3], ii) the so-called wedge plasmon polaritons [4] and iii) the domino plasmons [5], in which a periodic chain of metallic box-shaped elements protruding out of a metallic surface is able to support the propagation of very deep subwavelength confined electromagnetic modes. We will show how the concept of spoof surface plasmons can be also used to devise chiral surface plasmons that carry fractional angular momentum [6]: a helically-grooved metal wire can sustain spoof surface plasmon modes that have a chiral character.

References

[1] E. Moreno, F.J. Garcia-Vidal, S.G. Rodrigo, L. Martin-Moreno, and S.I- Bozhevolnyi, Opt. Lett. **31**, 3447 (2006).

[2] E. Moreno, S.G. Rodrigo, S.I. Bozhevolnyi, L. Martin-Moreno, and F.J. Garcia-Vidal, Phys. Rev. Lett. **100**, 023901 (2008).

[3] A. I. Fernandez-Dominguez, E. Moreno, L. Martin-Moreno and F. J. García-Vidal, *Phys. Rev. B* **79**, 233104 (2009).

[4] A. I. Fernandez-Dominguez, E. Moreno, L. Martin-Moreno and F. J. García-Vidal, *Opt. Lett.* **34**, 2063 (2009)

[5] D. Martin-Cano, M.L. Nesterov, A.I. Fernandez-Dominguez, F.J. Garcia-Vidal, L. Martin-Moreno and Esteban Moreno, *Opt. Express* **18**, 754 (2010).

[6] F. Ruting, A.I. Fernandez-Dominguez, L. Martin-Moreno and F.J. Garcia-Vidal (to be published).

The wire grid as a plasmonic reflective polarizer

Hristo S. Tonchev[1] and Olivier Parriaux[2]
[1] *Faculty of Physics, University of Sofia, Bulgaria*
[2] *Hubert Curien Laboratory UMR CNRS 5516, University of Lyon at Saint-Etienne, France*
parriaux@univ-st-etienne.fr

A subwavelength metallic grating can be a high extinction reflective polarizer if set at the condition of Fabry-Perot resonance for the plasmon mode propagating up and down the metal slits. Its features will be described and pending issues raised.

Introduction

Most applications of a subwavelength wire grid as a polarizer use it as a transmission polarizer. Some applications could draw configurational advantages from a reflective polarizer provided the reflection of the transmitted polarization can be damped to zero. A Fabry-Perot analogy for the TM_0 plasmon mode is constructed to establish this condition.

Results

The wire grid is composed of rectangular metallic lines on a substrate of index n_s with air in the slits as reproducibly fabricable by galvanic growth [1]. The period (Λ) to wavelength (λ) ratio fulfils the subcutoff condition of the +- 1st orders $\Lambda < \lambda/n_s$ that also makes the TE_0 evanescent in the grooves. Minimum TM reflection is obtained when the TM_0 Fabry-Perot resonance condition is satisfied:

$$2\beta h + \arg(r_s) + \arg(r_c) = 2m\pi \qquad (1)$$

$\beta = 2\pi n_e/\lambda$ (n_e is the TM_0 effective index and r_i are its reflection coefficients at the slit openings). We look for an analytical expression for all quantities involved in (1) to understand what it depends on. n_e can be easily found, but r_i can not despite the availability of an approximate expression by Lalanne et al. [2]. We thus opted for a breakdown of the problem already permitting to anticipate some interesting characteristics of such polarizer: Lyndin's true-mode method [3] delivers n_e and r_i of the TM_0 mode. The outcome of this analysis reveals the following interesting characteristics which will be developed and illustrated (Ref. figures hereunder showing TE and TM reflection):

- Zero TM reflection occurs at a grating depth ensuring quasi-zero TE transmission
- The condition of 0 TM reflection is weakly dependent of the period and metal type

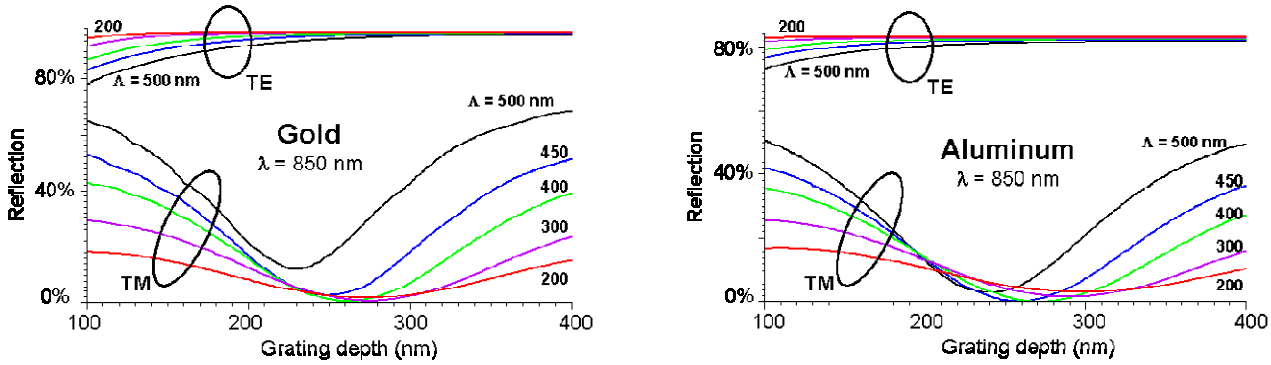

References

[1] F. Romanato, et al., *Appl. Opt.* **50**, 4529-4534 (2011)
[2] P. Lalanne, et al., *J. Opt. Soc. Am.* A 23, 1608-1615 (2006)
[3] N. Lyndin, www.mcgrating.com

Numerical solution of nonlocal hydrodynamic Drude model for arbitrary shaped nano-plasmonic structures using Nédélec finite elements

Kirankumar R. Hiremath[1], Lin Zschiedrich[2], Sven Burger[1,2], Frank Schmidt[1]
[1]*Computational Nanooptics Group, Konrad-Zuse-Zentrum für Informationstechnik Berlin, Germany*
[2]*JCMwave GmbH, Berlin, Germany*
hiremath@zib.de

The dispersive material properties of plasmonic structures are usually described by the Drude model and the Lorentz model. These material models take into account spatially *purely local* interactions between electrons and the light. Recent investigations have shown that these local models are inadequate as the size of the plasmonic scatterers become much smaller than the wavelength of the incident light [1, 2]. To overcome this, a sophisticated *nonlocal* material model is required, such as the hydrodynamic model of the electron gas [3].

The hydrodynamic model is formulated by coupling macroscopic Maxwell's equations with the equations of motion of the electron gas. This gives rise to a hydrodynamic polarization current. Considering only the kinetic energy of the free electrons, it yields the nonlocal hydrodynamic Drude model, which is given in frequency domain by a coupled system of equations

$$\nabla \times \mu_0^{-1}(\nabla \times \boldsymbol{E}(\boldsymbol{r},\omega)) - \omega^2 \varepsilon_0 \varepsilon_{\mathrm{loc}}(\boldsymbol{r},\omega)\boldsymbol{E}(\boldsymbol{r},\omega) = i\omega \boldsymbol{J}_{\mathrm{HD}}(\boldsymbol{r},\omega), \quad (1)$$

$$\beta^2 \nabla(\nabla \cdot \boldsymbol{J}_{\mathrm{HD}}(\boldsymbol{r},\omega)) + \omega(\omega + i\gamma)\boldsymbol{J}_{\mathrm{HD}}(\boldsymbol{r},\omega) = i\omega\omega_{\mathrm{p}}^2 \varepsilon_0 \boldsymbol{E}(\boldsymbol{r},\omega), \quad (2)$$

where $\boldsymbol{E}$ is the electric field, $\boldsymbol{J}_{\mathrm{HD}}$ is the hydrodynamic current, $\varepsilon_{\mathrm{loc}}$ is the relative permittivity due to the local-response, β^2 is a term proportional to the Fermi velocity, γ is the damping constant, and $\omega_{\mathrm{p}}^2 = \frac{e^2 n_0}{\varepsilon_0 m_{\mathrm{e}}}$ is the plasma frequency of the free electron gas.

Nonlocal material response distinctively changes the optical properties of nano-plasmonic scatterers and waveguides, e.g. as shown in the accompanying figure, for a cylindrical nanowires nonlocality generates characteristic resonances *(only) beyond* the plasma frequency ($\omega/\omega_p > 1$).

Recent works encountered difficulties in dealing with the grad-div operator in Eq. (2). Therefore, in these studies the model has been simplified with the curl-free hydrodynamic current approximation [4], which causes spurious resonances, e.g. resonances of cylindrical nanowires for $\omega/\omega_p < 1$.

In this work we present a rigorous weak formulation of Eqs. (1)-(2) in the Sobolev spaces $H(\mathrm{curl})$ for the electric field and $H(\mathrm{div})$ for the hydrodynamic current, which directly leads to a consistent discretization based on Nédélec's finite element spaces [5]. Comparisons with Mie theory results agree well (see the figure.). We also demonstrate the capability of the method to handle any arbitrarily shaped scatterer.

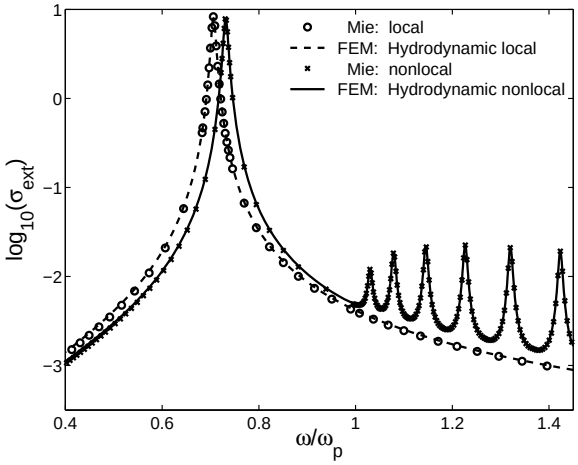

References

[1] R. Ruppin. *Opt. Commun.*, 190(1-6):205–209, 2001.
[2] S. Palomba, L. Novotnyb, and R. E. Palmer. *Opt. Commun.*, 281(3):480–483, 2008.
[3] A. D. Boardman. *Electromagnetic surface modes*, pages 1–76. John Wiley and Sons Ltd., 1982.
[4] J. M. McMahon, S. K. Gray, and G. C. Schatz. *Phys. Rev. B*, 82:035423, 2010.
[5] K. R. Hiremath, L. Zschiedrich, and F. Schmidt. arXiv:1201.1527v2 (submitted to *J. Comp. Phys.*), 2012.

Angularly robust resonant reflection by grating-induced mode coalescence

Alexandre V. Tishchenko and Olivier Parriaux
Hubert Curien Laboratory UMR CNRS 5516, University of Lyon at Saint-Etienne, France
parriaux@univ-st-etienne.fr

A very high index contrast dual-mode slab waveguide having a deep corrugation at both sides exhibits under normal incidence a wide angular spectrum resonant reflection compatible with LED beams.

Introduction

Resonant (or abnormal) reflection has so far been used for the processing of narrowband, spatially coherent beams [1]. Special waveguide grating structures have been designed to keep a narrow reflection peak with a slightly focused beam [2,3] but no resonant reflection element has been proposed that can process a LED beam of wide wavelength and angular spectra: there is always around normal incidence a reflection peak splitting spoiling the transmission/reflection contrast. We show here that mode coalescence in a dual-mode slab waveguide caused by a deep two-side corrugation endows resonant reflection with a property of high angular robustness.

Results

The theoretically simulated grating waveguide structure is a slab waveguide of amorphous Silicon (a-Si, 3.7 index) deposited on a fused quartz substrate with air overlay. The substrate is sinusoidally undulated, the a-Si-air interface also, conformally. The waveguide thickness is just above the cutoff thickness of the TE_1 mode at the wavelength of interest $\lambda = 850\ nm$. An interesting numerical experiment is to scan the grating period at constant wavelength and waveguide thickness under normal incidence with the undulation depth as a parameter. The left figure reveals that the effective index of the TE_0 and TE_1 modes, which are well separated at shallow grating depth, each exhibiting its narrow reflection peak, merge with increasing depth. Taking now the period corresponding to the excitation of the coalesced mode (380 nm) and the corresponding grating depth (135 nm) gives the spectrum of the right figure with the incidence angle as a parameter and demonstrates that the angular acceptance is in the form of a wide plateau (the peak splitting has disappeared), and is as wide as 15 degrees without notable alteration of the reflection spectrum. Thus, abnormal reflection is now available to process low coherence beams in the red, near-IR thanks to the existence of the highly transparent PECVD a-Si of solar cells.

The presentation will give a phenomenological understanding of the effect and confirm it on the basis of an analytical Rayleigh approximation.

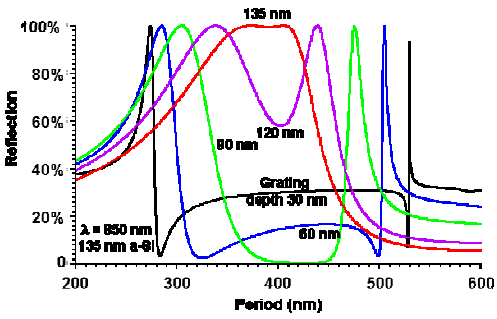

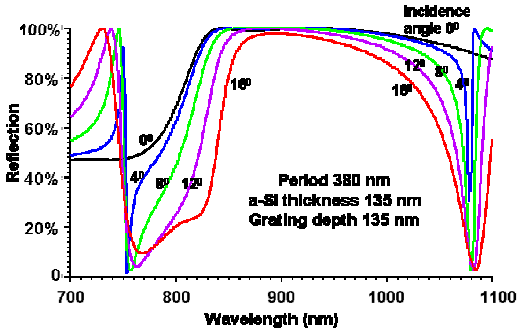

References

[1] G. A. Golubenko et al., Sov. J. Quantum Electron. **15**(7), 886–887 (1985).
[2] E. Bonnet et al., Opt. & Quant. Electron., **35**, 1025-1036 (2003)
[3] F Lemarchand and A. Sentenac, Opt. Lett. **23**, 1149–1151 (1998).

Modeling reflections induced by waveguide transitions

D. Melati, F. Morichetti, and A. Melloni
Dipartimento di Elettronica e Informazione, Politecnico di Milano, via G. Colombo 81, 20133 Milano, Italy
melloni@elet.polimi.it

A simple and fast model to describe reflection induced by lumped waveguides discontinuities is presented. Model is applied to fabricated structures and compared with measurements and electromagnetic simulations.

Summary
Interfaces between different optical waveguides generate undesired reflections which may result in detrimental effects and deterioration of the circuit performances. In this work we propose a fast numerical model to quantify the reflection coefficient induced by sharp variations of the waveguide geometry. The model is based on the Fresnel reflection coefficient, holds for straight waveguides and for a discontinuity plane orthogonal to the propagation direction. It is assumed that the field at the interface between waveguide 1 (incoming) and 2 (outgoing) can be approximated with the mode of the waveguide 1. Exploiting a perturbative approach the phase effective index $n_{eff\,2(1)}$ at the beginning of waveguide 2, as seen from waveguide 1, is given by

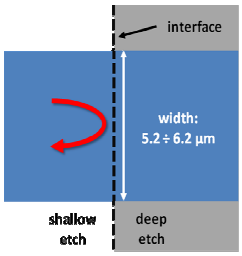

Fig 1: Picture of the transition. Red arrow points out the considered reflection.

$$\frac{\int \varphi_1^*(x,y)\left(\nabla_\tau^2\varphi_1(x,y)+\kappa_0^2 n_2^2(x,y)\varphi_1(x,y)\right)dxdy}{\int \varphi_1(x,y)\varphi_1^*(x,y)dxdy}=\left(\frac{2\pi}{\lambda}n_{eff\,2(1)}\right)^2 \qquad (1)$$

where φ_1 is the mode of the incoming waveguide and n_2 is the index profile of the outgoing waveguide. The reflection coefficient is then defined as $R=(n_{eff\,1}-n_{eff\,2(1)})/(n_{eff\,1}+n_{eff\,2(1)})$ with $n_{eff\,1}$ the effective index of the mode of the first waveguide.

The proposed model has been applied to the transition section shown in fig. 1, realized in InP technology (air confined waveguide with core-substrate index contrast of 2.7%). At the transition, etch depth is abruptly changed from 200 nm to 1.7 µm and various transition sections are designed changing the waveguide width from 5.2 µm to 6.2 µm. Reflections induced by these discontinuities have been also measured through OFDR technique setup [1]. Fig. 2 shows the agreement between experimental results (diamonds) and the described model (blue dashed line), the latter predicting both the reflection decrease versus waveguide width and the absolute value of the power reflection. Electromagnetic simulations based on Eigenmode Expansion method [2] were performed (red dashed line) and results are in good accordance with measurements and with proposed model. While direct electromagnetic simulations take about one hour per data point, the described model requires only some minutes to compute the modes and to evaluate $n_{eff\,2(1)}$ by eq. (1), with a great saving in time and resources.

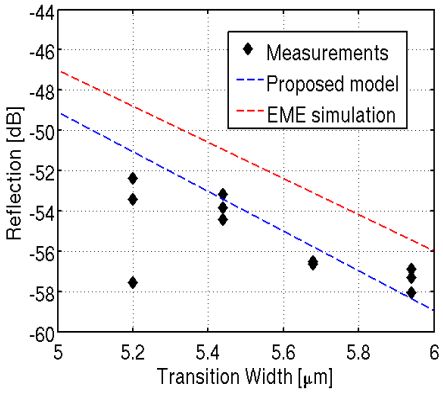

Fig 2: Reflection of waveguide transition for different widths: measurements (diamonds), proposed model (blue dashed line) and EM simulation (red

References

[1] U. Glombitza, E. Brinkmeyer, "Coherent frequency-domain reflectometry for characterization of single-mode integrated-optical waveguides", Journal of Lightwave Technology, vol.11, no.8, Aug. 1993
[2] D.F.G. Gallagher, T.P. Felici, "Eigenmode Expansion Methods for Simulation of Optical Propagation in Photonics – Pros and Cons." Proc. SPIE, vol 4987, pp.69-82, 2003

Tailored Design for WDM Filters in BCB-embedded PhC Membranes

Stefania Malaguti[1], Gaetano Bellanca[1], Stefano Trillo[1],
Luisa Ottaviano[2], Kresten Yvind[2], Sylvain Combrié[3] and Alfredo De Rossi[3]
[1] *Department of Engineering, University of Ferrara, via Saragat 1, 44122 Ferrara, Italy*
stefania.malaguti@unife.it
[2] *DTU Fotonik Ørsteds Plads, Bygning 345v, 2800 Kgs. Lyngby, Denmark*
[3] *Thales Research and Technology, Route Departementale 128, 91767, Palaiseau, France*

We propose a design strategy for WDM filters in BCB-embedded Photonic Crystal membranes which overcomes the issues related to the weaker vertical optical confinement introduced by the cladding material.

Introduction

Photonic Crystals (PhCs) are increasingly used for the realization of compact optical components. Among different possible PhC structures, two-dimensional PhC (2D-PhC) slabs have attracted great attention for their relatively easy fabrication. These devices confine the light on the propagation plane through the Photonic Band Gap (PBG) effect. The vertical confinement, on the contrary, is provided by the large refractive index contrast between the slab and the cladding, and is maximized by realizing suspended vertical PhC membranes in air [1]. Unfortunately, this solution lacks of mechanical robustness and a supporting material in one or both sides of the membrane is often introduced, although the well-known issues (decrease of the quality factor Q, losses due to vertical radiation, reduced transmission bandwidth for PhC waveguides, etc.) related to the weaker vertical optical confinement. In this work we propose a design procedure for WDM filters on BCB-bonded PhC membranes realized on quaternary semiconductor materials.

Results

The first step of the proposed approach is the optimization of the PhC membrane parameters (period *a*, thickness *h*, radius of the holes *r*). As the filter is intended to be used in a WDM system, high Q and wide free spectral range (FSR) are desirable, to guarantee a channel separation which fits WDM specifications. In this work L*n* cavities (obtained by removing *n* adjacent holes from the PhC membrane) are considered. Suitable configurations for WDM filters are L5 and L7 cavities (respectively with 5 and 7 adjacent holes removed), which show a reasonable Q_0 (i.e. 30000÷70000 for the symmetrically embedded PhC membrane) and a still acceptable FSR (20 nm÷30 nm) [2]. Once optimized the PhC parameters, bus and drop waveguides can be properly introduced near the resonator. Accurate tailoring of the waveguide geometry should also be considered and is the fundamental key of the design procedure. In fact, by using a simple W1 PhC waveguide the resulting allowed bandwidth is very small, thus preventing the possibility to transmit the complete WDM channel frame. Wider transmission bands can be obtained by modifying the geometry of the waveguide. Other optimizations involve prevention of unacceptable losses for the waveguide propagation (i.e. irradiation into the cladding for frequencies above the light cone and scattering for frequencies in slow-light propagation regime) and identification of the most suitable coupling conditions with the cavity. Results will be presented and discussed.

The authors acknowledge EC funding under Copernicus Project.

References

[1] J.D. Joannopoulos et al., Photonic Crystals Molding the Flow of Light, Princeton University Press, ISBN: 9780691124568, 2008

[2] M. Okano et al, J. Opt., **12**, 075101 (2010) and M. Okano et al, J. Opt., **12**, 015108 (2010)

Local Boundary Condition for Terminating Photonic Crystal Waveguides

Zhen Hu[1] and Ya Yan Lu[2]

[1]*Department of Mathematics, Hohai University, Nanjing, Jiangsu, China*
[2]*Department of Mathematics, City University of Hong Kong, Kowloon, Hong Kong*

In numerical simulations of photonic crystal (PhC) devices, artificial boundary conditions are needed to terminate the PhC waveguides which serve as the input and output ports. The rigorous boundary condition is nonlocal. A local boundary condition is formulated and illustrated by examples.

Introduction

A PhC device is often connected by a few PhC waveguides that serve as the input and output ports. Numerical simulations for such a device require artificial boundary conditions to terminate the PhC waveguides. A rigorous boundary condition for terminating a PhC waveguide is available [1]. It it is a nonlocal condition that connects the wave field at different points on a line or plane (for 2D or 3D structures, respectively) perpendicular to the waveguide axis. For pure 2D structures, the nonlocal boundary condition is still very efficient, but for 3D structures, it becomes too expensive to use. In the following, we develop a simple local boundary condition.

Consider a semi-infinite PhC waveguide given in $x < x_0$, where the waveguide axis is parallel to the x axis. Let $\phi_l^+(x,y)e^{i\beta_l x}$ and $\phi_l^-(x,y)e^{-i\beta_l x}$, $1 \le l \le l_*$, be the incoming and outgoing propagating Bloch modes of the waveguide, where l_* is the total number of propagating modes and β_l is real. If the line $x = x_0$ is sufficiently far away from the center of the device, the evanescent modes in the waveguide can be ignored, then the wave field in the waveguide can be approximated by $u \approx u^{(i)} + \sum_{l=1}^{l_*} b_l \phi_l^-(x,y)e^{-i\beta_l x}$, where b_l for $l = 1, 2, .. \ l_*$, are the unknown coefficients and $u^{(i)}$ may consist of only one incoming mode. A local boundary condition can be derived by eliminating the unknown coefficients. Let the period of the PhC waveguide be a and let $\prod_{l=1}^{l_*}(1-\xi e^{i\beta_l a}) = 1 + B_1\xi + B_2\xi^2 + \cdots + B_{l_*}\xi^{l_*}$, then the local boundary condition is

$$u_0 + B_1 u_1 + \cdots + B_{l_*} u_{l_*} = u_0^{(i)} + B_1 u_1^{(i)} + \cdots + B_{l_*} u_{l_*}^{(i)},$$

where $x_l = x_0 + la$, $u_l = u(x_l, y)$ and $u_l^{(i)} = u^{(i)}(x_l, y)$.

Results

Consider a 90° bend in a square-lattice PhC similar to the one studied in [2], but the dielectric constant and the radius of the rods are $\varepsilon = 10$ and $r = 0.375a$, where a is the lattice constant. For frequency $\omega a/2\pi c = 0.785$, there are two propagating modes in the waveguide. Let the computational domain be a square with $m \times m$ unit cells, and N be the number of sampling points on each edge of the unit cells. With the nonlocal boundary condition of [1], we obtain a transmission coefficient $T = 0.546$ for $m = 11$ and $N = 13$. For the same N and local boundary condition, we have $T = 0.535$, 0.543 and 0.546 for $m = 11$, 13 and 15, respectively. Therefore, we can obtain reasonably accurate solutions using the local boundary condition, if we increase the computational domain by a few lattice constants in each direction.

Acknowledgments

The work is partially supported by the National Science Foundation of China (project 11101122) and the Fundamental Research Funds for Central Universities of China (project 2009B05514).

References

[1] Z. Hu, Y. Y. Lu, Opt. Express. 16, 17383-17399 (2008).
[2] A. Mekis, S. H. Fan, J. D. Joannopoulos et. al, Phys. Rev. Lett. 77, 3787-3790 (1996).

Analytical approach towards fishnet negative index of refraction

Jan Fiala, Pavel Kwiecien, and Ivan Richter
Czech Technical University in Prague, Faculty of Nuclear Sciences and Physical Engineering
Department of Physical Electronics, Brehova 7, 11519 Prague 1, Czech Republic
jan.fiala@fjfi.cvut.cz, richter@fjfi.cvut.cz

Introduction

Although rigorous computation necessary for detailed simulations of wave interactions with plasmonic / metamaterial structures is already quite easily achievable on fast computers with optimized numerical methods nowadays, the appliance of meaningful (quasi)analytical models provides much more physical insight, with respect to applications. This work is dedicated to the analytical approach able to model effective (negative index) properties in metamaterial structures; the motivation towards these studies being in our parallel experimental activities aiming towards structure realization, mainly based on either self-assembly or biomimetic techniques, oriented into such application areas as surface-plasmon resonance biosensing and/or surface-enhanced Raman spectroscopies.

Analytical model of metamaterial structures

Based on our previous experience with simpler sub-λ plasmonic structures [1], we have recently applied, inspired with [2], the intuitive wave-contribution technique to achieve and understand the mechanism of more complex behavior of negative effective refractive index in fishnet metamaterial structures, i.e. multilayer metal-insulator-metal structures with periodic vertical nanohole arrays [3,4]. While deriving the model, the original assumption, applicable in purely plasmonic structures, allowing the energy to propagate only in the vertical direction of aperture orientations, had to be generalized since such a structure also acts as a plasmonic waveguide in the horizontal direction. By coupling all the wave contributions and applying the periodicity conditions for the plasmonic field amplitudes in the perpendicular direction, the relevant field amplitudes of the Bloch modes have been found to be dependent on the plasmonic diffracted field via one scattering coefficient only. Additionally, the periodicity condition for the field amplitudes of the Bloch modes, obtained in such a way, already contains the effective negative-index information. Thus, in this way, we have been able to achieve the complex dispersion equation which solution provides the required complex refractive index. Since the appropriate scattering coefficients cannot be simply evaluated with the analytical approach, we have also used both our in-house efficient implementations of the Fourier modal methods (i.e. periodic 2D rigorous coupled-wave analysis - RCWA / aperiodic 3D aRCWA) as well as 3D Meep FDTD engine to calculate the respective field amplitudes and phases. Naturally, these techniques have been simultaneously applied for comparison of the approximate results of the negative refractive index, too.

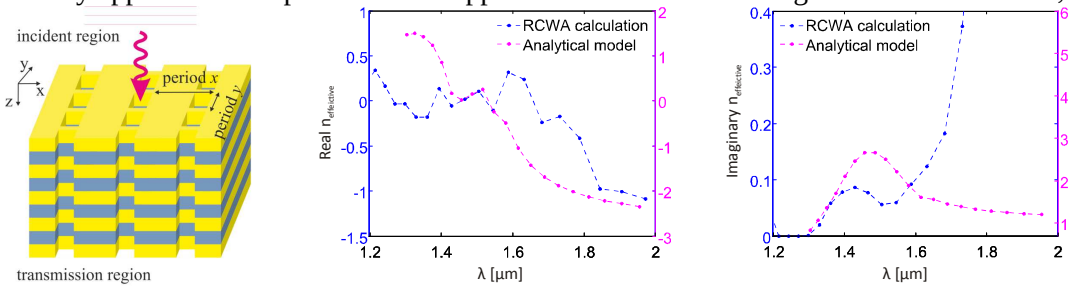

a) b) c)

Fig. a) Schematic picture of fishnet metamaterial structure and the spectral dependences of b) the real part and c) the imaginary part of effective refractive indices; comparison of RCWA and analytical model calculations.

Acknowledgements. The support of the Czech Science Foundation projects P205/10/0046 and P205/12/G118, as well as the Ministry of Education, Youth and Sports of the CR project OC09038 (COST MP0702 Action) is acknowledged.

References

[1] J. Fiala, I. Richter, *Optical and Quantum Electronics*, **41**, 409-427 (2009).
[2] H. Liu, P. Lalanne, *Nature*, **452**, 728-731 (2008).
[3] J. Fiala, P. Kwiecien, I. Richter, J. Čtyroký, M. Šiňor, I. Richter, *SPIE Optics + Optoelectronics 2011* (April 2011, Prague, Czech Republic), 2011.
[4] J. Fiala, P. Kwiecien, M. Šiňor, I. Richter, paper JWA37, *FiO OSA Annual Meeting* (October 2011, San Jose, USA, 2011).

Simulation of optical forces on a microparticle on an optical waveguide

Olav Gaute Hellesø and Pål Løvhaugen
Dept. of Physics and Technology, University of Tromsø, 9037 Tromsø, Norway
olav.gaute.helleso@uit.no

Optical forces on microparticles (1-6μm diametre) have been calculated with Comsol Multiphysics. Different waveguide structures and microparticles have been studied. Conditions for stable trapping have been found. The numerical model will be described.

Introduction

The evanescent field of an optical waveguide can be used to trap micro- and nanoparticles [1]. On a straight waveguide, particles are propelled along the waveguide and attracted towards the centre of the waveguide surface. Different three-dimensional models have been implemented in Comsol Multiphysics, which uses the finite element method to calculate the field distributions. Integrating Maxwell's stress tensor over a particle's surface gives the optical force on the particle.

Results

For microspheres, the optical forces increase monotonically with the diametre for the sizes considered, which do not exhibit whispering gallery modes. We have also studied hollow glass spheres [2]. These can be trapped or repelled depending on the thickness of the shell. Both experimental trapping and simulating the forces on red blood cells is challenging because the refractive index of the cells is close to that of the surrounding media (water) and the cells are rather large (8μm diametre). We have studied the forces as function of the refractive index for smaller spheres (2 μm diametre) as this is simpler than for a full size cell. As the cells are elastic, they deform due to the optical pressure. We will present some initial results on deformation.
If the waveguide is terminated abruptly, light will diverge strongly out from the waveguide end (Fig. 1). We have found that this divergence is sufficiently large to trap small polystyrene spheres (1 μm diametre) about 1 μm from the end of the waveguide, while larger spheres (5 μm diametre) are pushed away. Two opposing waveguide ends give two counter-propagating fields that induce interference in the gap between the waveguide ends. The interference pattern can trap both small and larger spheres at several locations.
The finite element method is a powerful tool, but requires large amounts of memory for three-dimensional models. Optimization of the mesh is important to balance accuracy and memory use. The models have been run on a computer cluster, mostly using 64 processors and 128 GB RAM.

References

[1] B.S. Ahluwalia et al, "Optical trapping and propulsion of red blood cells on waveguide surfaces", Optics Express, Vol. 18, Issue 20, pp. 21053-21061 (2010).

[2] B.S. Ahluwalia, P. Løvhaugen and O.G. Hellesø, "Waveguide trapping of hollow glass spheres", Optics Letters, Vol. 36, Issue 17, pp. 3347-3349 (2011).

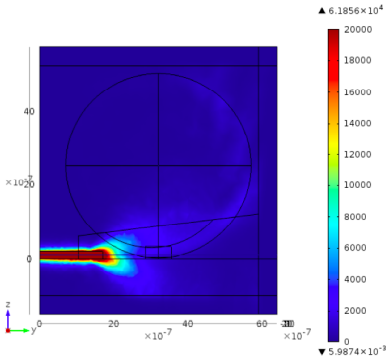

Figure 1 Scattering from a sphere at the end of an optical waveguide.

Modelling of Nanoparticle Arrays in Si Solar Cells

Reinhard Carius[1], Dirk Michaelis[2], Etienne Moulin[1], Ulrich Paetzold[1], and Christoph Wächter[2]

[1] *IEK5-Photovoltaik, Forschungszentrum Juelich GmbH, D-52425 Juelich, Germany,*

[2] *Fraunhofer Institute for Applied Optics and Precision Engineering, Albert-Einstein-Straße 7, 07745 Jena, Germany*

christoph.waechter@iof.fraunhofer.de

Targeting at the efficiency enhancement of Si solar cells effects of different geometries of particles and arrays consisting thereof residing at particular positions within the layer stack are investigated.

Introduction

Light-trapping effects are well suited to enhance the absorption efficiency of optically thin Si-layers, relying on either regularly [1] or randomly textured interfaces [2]. Due to the internal interplay of the impinging electromagnetic field and local charge oscillations metallic nano-structures can act as highly efficient scatterers. This way, plasmonics may improve absorption in solar cells, [3], although losses in the metal can be detrimental. In this contribution solar cell structures including nano-particle arrays embedded in the plane layer structure, Fig.1 a), as well as structures with reflection grating back contacts with quasi-conformal layer growth on top, Fig. 1 b), are analyzed.

a) 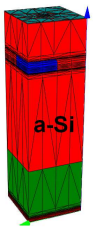

b) 

Fig.1: sketch of geometries under consideration
a) metallic nano-particle situated in the a-Si layer, quarter unit cell shown
b) textured substrate covered with metallic reflector and subsequent layer stack of a µc-Si cell

Results

Detailed numerical investigations of the different solar cell structures are performed on the basis of a rigorous fully 3-D finite element based Maxwell solver [4]. Variations of particle shape, size, position within the layer stack, and array period allow identifying configurations with increased absorption efficiency. This enhanced absorption is the result of a fairly complex interplay of reflection and transmission, guided modes and grating resonances. For the a-Si cell type efficiency enhancements up to 20% compared to a planar solar cell can be estimated. Furthermore, for the structured back reflector configuration an enhancement compared to conventional random texture light trapping is predicted, which could be experimentally approved, effectively, [5].

Support of this work by the German Federal Ministry of Education and Research (BMBF) within the project SunPlas (FKZ 03SF0354-B and -D) is gratefully acknowledged.

References

[1] M.T. Gale, et al., SPIE Vol. 1272, 60-66 (1990)

[2] M.Zeman, et al., Solar Energy Materials & Solar Cells 66, 353-359 (2001)

[3] H. A. Atwater, and A. Polman, Nature Materials, 9, 205-213 (2010)

[4] JCMsuite by JCMwave GmbH, www.jcmwave.com

[5] U. Paetzold et al., Applied Physics Letters, 99, 181105 (2011)

Fast Thermo-Optic Wavelength Scanning for Sensors Interrogation in SOI Technology

Andrey V. Tsarev[1], Francesco De Leonardis[2] and Vittorio M. N. Passaro[2]
[1]*Laboratory of Optical Materials and Structures, A.V. Rzhanov Institute of SB RAS, Novosibirsk, 630090, Russia*
tsarev@isp.nsc.ru
[2] *Photonics Research Group, Dipartimento di Elettrotecnica ed Elettronica Politecnico di Bari, 70125 Bari, Italy – passaro@deemail.poliba.it*

Introduction

The efficient interrogation of optical sensors by thermo-optic fast tunable filters with multiple partially reflected slanted mirrors in SOI waveguide structure has been studied by 2D FDTD and FEM. The 1 cm long device provides 1 pm wavelength resolution and 1 ms scanning over 40 nm range at 1550 nm.

Results

This paper proposes the interrogation of optical sensors by novel thermo-optic fast tunable filters with multiple partially reflected slanted mirrors in silicon-on-insulator (SOI) technology [1]. The tunable filter is used both for tunable band selection of broadband light source for interrogating the optical sensors, as well as for precise detection of interrogation optical wavelength [2]. New interrogator design is numerically studied for a compact structure by 2D FDTD and FEM. Here the optical sensor is modeled as a vertical Fabry-Perot (FP) filter (see ellipse in the left corner of Fig. 1), constituted by two strong parallel mirrors, with an additional 45° partial reflector [2]. This compact 1 cm device on SOI could provide sensor interrogation within the full 40 nm band (around 1550 nm) with 1 ms readout time, one per second speed and average heating power less than 16 mW.

The authors thank Company RSoft Design Group, Inc. and Company Comsol Inc. for providing commercial software for FDTD and FEM simulations.

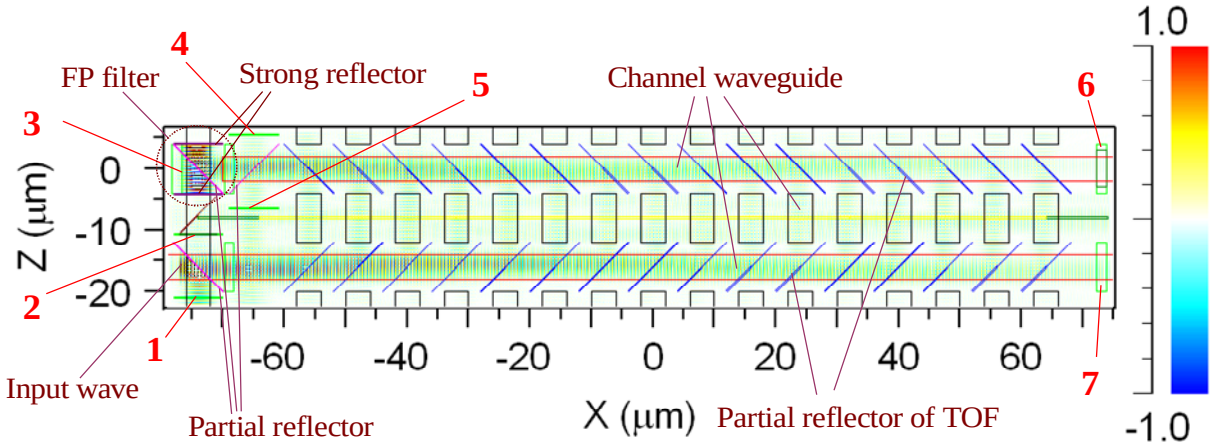

b)

Fig.1. Novel interrogator on SOI structure and optical propagation through FP sensor and multi-reflector interrogator on SOI with 16 partial reflectors. 2D FDTD simulation. Numbers indicate power monitors.

References

[1] F. De Leonardis, A. V. Tsarev, and V. M. N. Passaro, *Opt. Express*, **16**, 21333–21338 (2008).
[2] A. V. Tsarev, F. De Leonardis, and V. M. N. Passaro, *Opt. Lett.*, **36**, 3756-3758 (2011).

A Multiscale FEM for 2D Photonic Crystal Bands

Holger Brandsmeier[1] , Kersten Schmidt[2], Christoph Schwab[1]
[1] *Seminar für Angewandte Mathematik, ETH Zürich, Switzerland*
[2] *DFG Research Center Matheon, Technische Universität Berlin, Germany*
holger.brandsmeier@sam.math.ethz.ch

A Multiscale Finite Element Method (MSFEM) for high frequency wave propagation in Photonic Crystals (PhC) structures will be presented [1].

The MSFEM uses two-scale basis functions inside the PhC. As micro functions we use Bloch modes, which are computed as FEM solutions for a fully periodic PhC [7]. The macro functions are piecewise polynomials of degree p^{mac} which are supported over many periods of the crystal. We will numerically show that such a multiscale basis is very efficient as only a constant number of these functions are needed to simulate arbitrary large, finite PhCs with a constant L_2-error. In contrast, for standard discretisation schemes like FD, PWM, h- or p-FEM more and more basis functions are required when the number of scatterers increases inside the computational domain. We will explain how to use this multiscale basis to construct a conforming FEM which is coupled to a discretisation of the exterior domain. In particular, we will show how to numerically integrate the highly oscillatory two-scale functions with constant computational effort. We will verify the properties of the MSFEM by numerical experiments for PhC bands (see figure), an infinite band of locally-periodic dielectric scatterers in 2D.

References

[1] Brandsmeier, H., Schmidt, K., and Schwab, C. A Multiscale hp-FEM for 2D Photonic Crystal Bands.
[2] Hou, T., and Wu, X. A multiscale nite element method for elliptic problems in composite materials and porous media. Journal of Computational Physics 134, 1 (1997), 169-189.
[3] Matache, A. Sparse Two-Scale FEM for Homogenization Problems. J. Sci. Comput. 17, 1 (2002),659-669.
[4] Matache, A., Babuska, I., and Schwab, C. Generalized p-FEM in homogenization. Numer. Math. 86, 2 (2000), 319-375.
[5] Melenk, J., and Babuska, I. The partition of unity nite element method: basic theory and applications. Comput. Methods Appl. Mech. Engrg. 139, 1-4 (1996), 289-314.
[6] Rüegg, A. W., Schneebeli, A., and Lauper, R. Generalized hp-FEM for lattice structures. Research report no. 2002-23, ETH Zurich, Seminar of Applied Mathematics, 2002.
[7] Schmidt, K., and Kauf, P. Computation of the band structure of two-dimensional Photonic Crystals with hp Finite Elements. Comput. Methods Appl. Mech. Engrg. 198 (2009), 1249-1259.

Floquet-Bloch Waves for TM-polarized Light in 1D Photonic Crystals

Gregory V. Morozov[1] and Donald W. L. Sprung[2]
[1] *Scottish Universities Physics Alliance (SUPA), Thin Film Centre, University of the West of Scotland, Paisley PA1 2BE, Scotland*
gregory.morozov@uws.ac.uk
[2] *Department of Physics and Astronomy, McMaster University, Hamilton L8S 4M1, Ontario, Canada*

Using binary and sinusoidal photonic crystals as an example, it is shown how to construct two independent Floquet-Bloch waves for TM-polarized light in a lossless 1D periodic structure. Particular attention is given to those special cases where only one Bloch wave develops inside the structure.

Introduction

Physical problems involving periodic variations often reduce to Hill's equation

$$\frac{d^2 f(z)}{dz^2} + a(z) f(z) = 0\,, \qquad a(z) = a(z+d)\,, \tag{1}$$

where $a(z)$ is a piecewise continuous, periodic, real or complex valued function of the real variable z. First introduced by Hill in 1877, this equation has appeared in many applications, including the propagation of electrons in crystals and semiconductor superlattices and the propagation of optic waves in photonic crystals. There is always one non-trivial particular solution $F_1(z)$ of Eq. (1), called a Floquet-Bloch wave, which satisfies the relation $F_1(z+d) = \rho_1 F_1(z)$, where ρ_1 is a non-zero, generally complex, constant. A second linearly independent particular solution constitutes either a second Floquet-Bloch wave, $F_2(z+d) = \rho_2 F_2(z)$ or a certain function $G(z)$, with the property $G(z+d) = \rho_1 G(z) + \rho_1 dF_1(z)$.

Results

In the recent paper [1], we showed in a transparent manner how to build Floquet-Bloch waves for TE-polarized light in lossless 1D binary photonic crystals for different bands of the frequency domain. Special attention was given to cases where the function $G(z)$ replaces one of the two Bloch waves. The purpose of this paper is to extend the results to TM-polarized light. As in Ref. [1], we use a binary photonic crystal as an example. However, we supplement that by constructing Bloch waves in a sinusoidal photonic crystal (rugate filter) as well. The TM case differs from TE in several ways. For a 1D photonic crystal with a real valued (no absorption) periodic refractive index, stratified in the z direction Maxwell's equations, in the case of TE polarized light of frequency ω reduce to Eq. (1) with $a(z)$ taking the form

$$a(z) = k^2 n^2(z) - \beta^2\,, \qquad n(z+d) = n(z)\,, \qquad k \equiv \omega/c \equiv 2\pi/\lambda\,, \tag{2}$$

where β is the (constant) x component of the wave vector of modulus $k\,n(z)$ inside the medium and $f(z)$ stands for the electric field $E(z)$. In the case of TM polarized light we end up with the equation for the magnetic field $H(z)$ involving a first derivative term

$$\frac{d^2 H(z)}{dz^2} + \left[k^2 n^2(z) - \beta^2\right] H(z) - \frac{2}{n(z)} \frac{dn(z)}{dz} \frac{dH}{dz} = 0\,, \qquad n(z) = n(z+d)\,. \tag{3}$$

That may lead to new features to be taken into consideration when constructing the Bloch waves and/or the function $G(z)$.

References

[1] G. V. Morozov and D. W. L. Sprung, EPL (Europhys. Lett.) **96**, 54005 (2011).

Efficient Boundary Integral Equation Method for Photonic Crystal Fibers

Wangtao Lu[1,2] and Ya Yan Lu[2]
[1] *University of Science and Technology of China, School of Mathematical Sciences, Hefei, China*
luwan@mail.ustc.edu.cn

[2] *City University of Hong Kong, Department of Mathematics, Kowloon, Hong Kong*

A new high order boundary integral equation (BIE) mode solver is developed for photonic crystal fibers with smooth interfaces. It solves only two functions on the interfaces. Numerical results indicate that the new BIE method achieves exponential convergence and extremely high accuracy.

Summary

Boundary integral equation (BIE) methods are suitable for analyzing photonic crystal fibers (PCFs), since they formulate eigenvalue problems only on the interfaces and are capable of computing leaky modes accurately. Existing high order BIE methods [1] give rise to $F(\beta)\phi = 0$, where the matrix F depends on β and ϕ represents four functions on the material interfaces. We develop an efficient high order BIE method that solves two functions on the interfaces. This implies that we can get the same level of accuracy with the size of $F(\beta)$ reduced by one half, leading to a significant reduction in the required computing time. The key step is to use the kernel-splitting technique for discretizing the hyper-singular boundary integral operators [2]. By computing the relations between $\{E_z, H_z\}$ and $\{H_x, H_y\}$ on the material interfaces, we establish the equation $F(\beta)\phi = 0$ where ϕ represents $\{H_x, H_y\}$. As an example, we calculate the fundamental mode for the PCF shown in Fig. 1. Numerical results for $\lambda = 1.51\mu m$ are

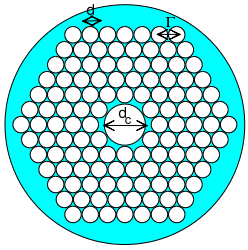

Fig. 1. Hollow core PCF with five rings of circular holes: the pitch is $\Gamma = 2.74\mu m$, the hole diameter is $d = 0.95\Gamma$ and the core diameter is $d_c = 2.5d$.

listed in the following table, where N_F is the size of $F(\beta)$. For comparison, Pone *et al* [1] gives

N_F	β/k_0
8360	$0.984516001097 + 3.41090\text{E}{-8}i$
12240	$0.984516000835 + 3.41133\text{E}{-8}i$
14640	$0.984516000835 + 3.41147\text{E}{-8}i$

$\beta/k_0 = \underline{0.9845159}74195 + \underline{3.4}3472\text{E}{-8}i$ for $N_F = 12544$.

References

[1] E. Pone, A. Hassani, S. Lacroix, A. Kabashin and M. Skorobogatiy, *Opt. Express* **15**, 10231–10246 (2007).
[2] R. Kress, *J. Comput. Appl. Math.* **61**, 345–360 (1995).

Mode Field Diameter of Index Guided Photonic Crystal Fibers

Dinesh Kumar Sharma and Anurag Sharma

Physics Department, Indian Institute of Technology Delhi, New Delhi-110016, India
dk81.dineshkumar@gmail.com, asharma@physics.iitd.ac.in

We use our earlier-developed analytical field model for the mode of index guided photonic crystal fibers to obtain various mode field diameters (MFDs) and examine the procedures for obtaining these experimentally.

Introduction

Mode field diameter (MFD) in an important parameter to characterize an optical fiber and has been used extensively for conventional fibers [1]. The same concepts have been extended to index guided photinc crystal fiber (PCFs); however, due to the non-Gaussian nature of the field and due to the non-circular symmetry of the field, a simple extension of these definitions has limited applicability. Using our earlier developed analytical field model [2], we have examined various methods and procedures to obtain MFDs. We present some results here.

Results

Typically, one defined three MFDs: Petermann-I, Petermann-II and the Gaussian. Difference between Petermann-I and Petermann-II MFDs shows the deviation of the field from the Gaussian nature and in most cases, the field of PCFs is non-Gaussian. Experimentally, however, most methods are based on the assumption of Gaussian variation of the field. For example, by scanning the near-field intensity along a diameter and by fitting a Gaussian in the obtained scanned values, MFD is obtained [3]. However, in this procedure, it is important to choose the diameter carefully as the MFD obtained could vary significantly with this choice as the field (and intensity) has significant azimuthal variation. Our field model [2] takes into account this variation well. Using this model, we have obtained various MFDs for LMA-8 and LMA-11 fibers [3]. The results are given in Fig. 1. These results show that experimental procedure, discussed above, can result in very different MFDs, if the scan axis ($\phi = 0$, $\phi = \pi/6$, or any angle in between) is not chosen properly. The results further show that Gaussian ($\phi = 0$) and Peterman-I are close to the experimental results while Gaussian ($\phi = \pi/6$) and Petermann-II are significantly different. This shows that the experimental results of [3] were obtained by scanning close to $\phi = 0$ axis and that is what should be done in an experiment to obtain the estimate of Petermann-I MFD. Further work is in progress to examine other experimental procedures.

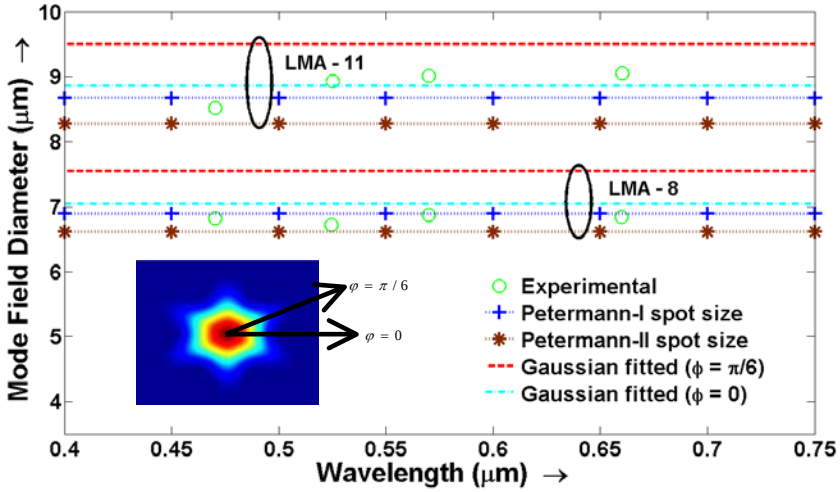

Fig. 1 Mode Field Diameter of PCFs as a function of wavelength

This work was supported by grant from the Council of Scientific and Industrial Research (CSIR), Govt. of India.

References

[1] M. Artiglia *et al.*, *Journal of Lightwave Technol.* **7**, 1139 (1989).
[2] A. Sharma and H. Chauhan, *Opt. Quantum Electron.* **41**, 235 (2009); Also *OWTNM 2009.*
[3] M.D. Nielsen *et al.*, *Opt. Exp.* **12**, 430 (2004).

Finite Element Analysis of Anisotropic Optical Waveguides with Arbitrary Optic-Axis Orientation

Hsuan-Hao Liu[1] and Hung-chun Chang[2]
[1] *Graduate Institute of Photonics and Optoelectronics, National Taiwan University, Taipei, Taiwan 10617, R.O.C.*
[2] *Department of Electrical Engineering, Graduate Institute of Photonics and Optoelectronics, and Graduate Institute of Communication Engineering, National Taiwan University, Taipei, Taiwan 10617, R.O.C.*
hcchang@cc.ee.ntu.edu.tw

A finite element formulation is developed to analyze anisotropic planar optical waveguides with an arbitrary permittivity tensor, such as those containing liquid crystals with arbitrary optic-axis orientation. One goal is to correctly determine the possible leakage losses of leaky modes.

Introduction

The simple planar optical waveguide, when composed of anisotropic slabs such as the birefringent $LiNbO_3$ and $LiTaO_3$ crystals, may possess complicated modal characteristics. For symmetric slab optical waveguides made of such crystalline media with the optic-axis orientations varying in the coplanar plane ($\phi = 90^o$ and θ varying in Fig. 1(a)), the eigenvalue equation was derived analytically in [1] for solving the modal propagation constant. Due to the general optic-axis direction, the TE and TM modes can couple with each other and the guided mode can couple to the radiating plane waves in the substrate, suffering leakage losses. The loss coefficient of such leaky mode versus the orientation angle of the optic axis as obtained from the imaginary part of the modal propagation constant was presented in [1]. In this paper, we develop a numerical eigenmode solver based on the finite element formulation for anisotropic planar optical waveguides with more general situations, i.e., the optic-axis orientation varying not only in certain planes but in an arbitrary manner. Waveguide layer containing liquid crystals or formed by liquid crystals is such example when their molecular directors can be freely controlled. Correct calculation of the complex modal propagation constant and thus the leakage loss is one of the main goals.

Results

A quadratic eigenvalue problem is formulated based on the finite element method (FEM) and solved using the shift-and-invert Arnoldi method. The anisotropic perfectly matched layers (PMLs) [2] are incorporated into the formulation to facilitate the computation of the complex modal propagation constant of the leaky mode. Agreement with the analytical analysis results for the leakage losses in [1] ($\phi = 90^o$) has been obtained as shown in Fig. 1(b) for the TE fundamental mode, and we are able to provide results for the more general cases involving arbitrary optic-axis orientations. One important finding is that the thickness of the PML needs to be carefully designed, possibly much larger than that conventionally used, to obtain correct leakage-loss values.

References

[1] D. Marcuse and I. P. Kaminow, *IEEE J. Quantum Electron.* **QE-15**, 92–101 (1979).

[2] F. L. Teixeira and W. C. Chew, *IEEE Microwave Guided Wave Lett.* **8**, 223–225 (1998).

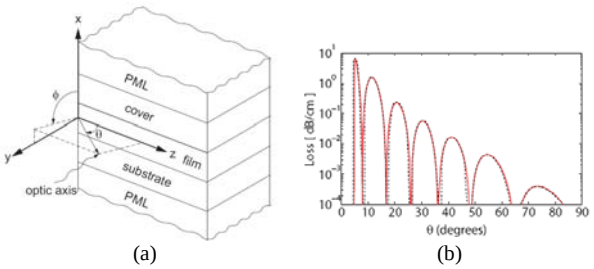

(a) (b)

Fig. 1. (a) Planar waveguide structure. (b) Results from [1] (black dotted) and this work (red) for calculated leakage loss vs. θ ($\phi = 90^o$) of the TE fundamental mode.

Waveguiding Properties of Ribbed Surface Waveguides in Three Frequency Domains

Christopher Alain Jones, Stefan Franz Helfert, Jürgen Jahns
Optical Information Technology, University of Hagen, Universitätsstrasse 27/PRG 58084 Hagen, Germany
Christopher.Jones@FernUni-Hagen.de

Properties of surface wave propagation along a longitudinally ribbed waveguide are examined in regards to the different geometrical parameters. A comparison between distinct frequency ranges is to be undertaken and the effect on both the transmittance and field reach are to be examined accordingly.

Introduction

Ribbed waveguides, as seen in Figure 1, are established structures in microwave technology. In the following the behavior of such structures is to be examined and compared over 3 distinct wavelength regions. Firstly the microwave domain around $\lambda_0 = 750\,\mathrm{mm}$, secondly the terahertz domain around $\lambda_0 = 750\,\mu\mathrm{m}$, where wave guiding is made possible by the inductive wave impedance of a ribbed surface and thirdly optical plasmon waves at $\lambda_0 = 750\,\mathrm{nm}$. It is of particular interest to see whether the influence of the geometry scales over the different frequency domains. Also the effect on wave attenuation and field reach into the surrounding dielectric media is to be examined. Especially in plasmonics it is usually the case that field reach and attenuation are inversely correlated, i.e. low attenuation usually coincides with large field reach. One possibility to reduce the dissipative losses could be to reduce the amount of metal in the core this can be achieved by ribbing the waveguide. The numerical results are computed with the Method of Lines [1], an eigenvalue method for partial differential equations. The metric by which the wave guiding performance is judged is the figure of merit $FoM = \frac{\tau}{\sigma^2}$, where $\tau = \frac{I(\Lambda)}{I(0)}$ is the transmittance over one period Λ and σ^2 the variance as gauge for the field reach of the transmitted Floquet mode.

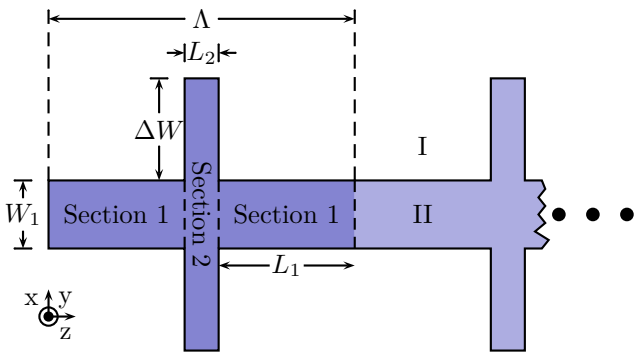

Figure 1: Ribbed plasmonic waveguide, gold II in dielectric I ($\varepsilon = 4$).

Results

The different geometrical parameters are varied within certain bounds and their effect on the figure of merit examined and compared between the three frequency domains. As example a plot showing the dependencies on distance between two ribs is shown on the right in Figure 2. Different effects are visible for one the clear distinction between the curves for the lower frequency domains compared to the optical domain. Also a clear dip for the different parameters at a value of roughly $L_1 = 85\,\mathrm{nm}$ caused by resonance effects between the propagated wave and the geometry. Further results and interpretations are to be discussed.

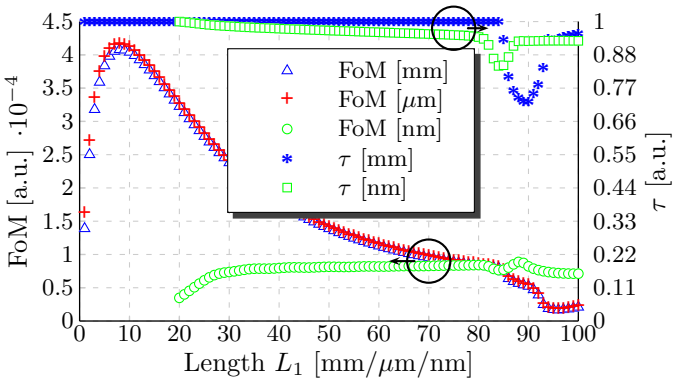

Figure 2: Figure of Merit and Transmittance plotted over the half distance between two ribs.

References

[1] Reinhold Pregla. Analysis of Electromagnetical Fields and Waves. John Wiley & Sons, Ltd., 2008.

Simulation of Reflection in Volume Bragg Grating and Tilted Fiber Bragg Grating Structures using a Bidirectional Split-Step Finite Difference Method

Debjani Bhattacharya and Anurag Sharma
Physics Department, Indian Institute of Technology Delhi, New Delhi-110016, India
asharma@physics.iitd.ac.in, debjani112@gmail.com

We present the results of simulation of reflections in a tilted fiber Bragg grating and in a volume Bragg grating obtained using our finite difference split step nonparaxial (FDSSNP) propagation method.

Introduction and Results

Numerical modeling of reflection requires methods, which can model both the forward and backward propagating fields. Methods like the finite difference time domain (FDTD) method are computationally very extensive. On the other hand the beam propagation method (BPM) is inherently unidirectional, although can be made bidirectional iteratively [1]. Recently we have developed a finite difference based split-step nonparaxial (FDSSNP) method, which is bidirectional and can be used for treating reflections efficiently [2]. In this method, the second order scalar wave equation is solved directly. Both the forward and backward propagating fields are present in the solution. The forward and backward fields at any plane can be obtained from the total field and its z-derivative using the following relation,

$$\begin{bmatrix} \psi_+(z) \\ \psi_-(z) \end{bmatrix} = \begin{bmatrix} \frac{1}{2}\mathbf{I} & \frac{i}{2}\sqrt{\mathbf{S}_z^{-1}} \\ \frac{1}{2}\mathbf{I} & -\frac{i}{2}\sqrt{\mathbf{S}_z^{-1}} \end{bmatrix} \begin{bmatrix} \psi(z) \\ \psi'(z) \end{bmatrix} \qquad (1)$$

where S_Z is a matrix representation of the operator $\partial^2/\partial x^2 + k_0^2 n^2(x,z)$. We present here simulations of a tilted fiber Bragg grating (TFBG) and a highly reflecting volume Bragg grating (VBG). Figure 1 shows the spectrum of a TFBG, as expected the reflectivity decreases with increasing tilt angle. In Fig.2, the spectrum of a VBG is plotted for different incident Gaussian beam waist radius. The VBG considered in [3] has been used for comparison. Our results (*) compare well with the experimental and theoretical results given in [3]. Further work in progress and will be presented at the workshop.

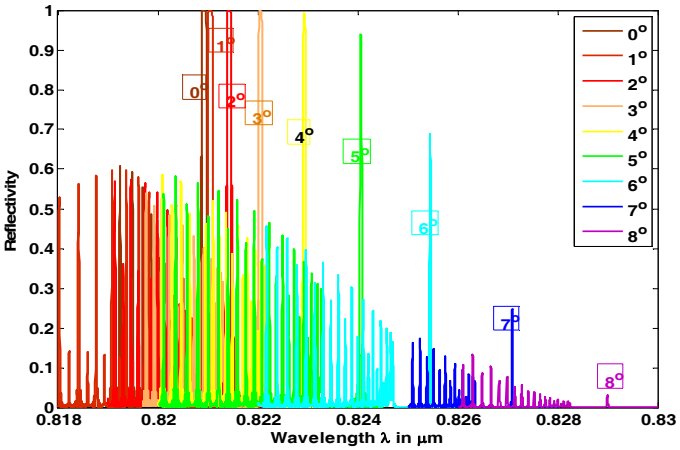

Fig.1: Spectrum of a TFBG

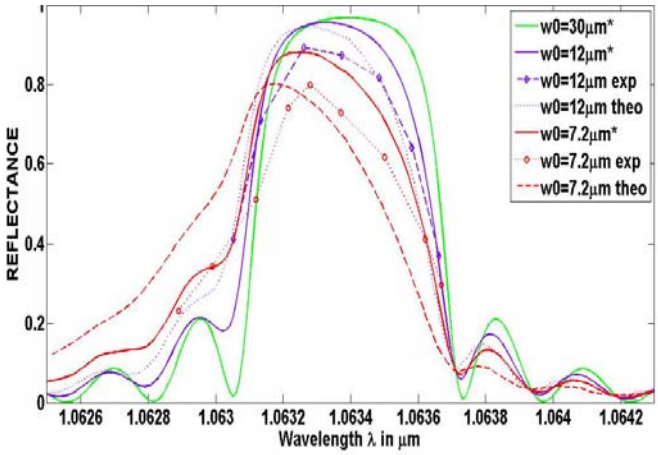

Fig.2: Spectrum of VBG for different beam waist radius.

The work was partially supported by the Council of Scientific & Industrial Research, Govt. of India.

References

[1] H.L. Rao, R. Scarmozzino, R.M. Osgood Jr., *IEEE Photon. Technol. Lett.* **18**, 830 (1999).
[2] A. Sharma, A. Agrawal, *Opt. Quantum Electron.* **38**, 19 (2006).
[3] J.E. Hellstrom, B. Jacobsson, V. Pasiskevicius and F. Laurell, *IEEE J. Quantum Electron.* **44**, 81 (2008).

Efficient analysis of bent waveguides with Fourier modal methods

Luis Zavargo-Peche[1], Jiří Čtyroký[2], Alejandro Ortega-Moñux[1], J. Gonzalo Wangüemert-Pérez[1] and Íñigo Molina-Fernández[1]

[1] *Communications Eng. Dept., Malaga University, Campus de Teatinos, 29071 Malaga, Spain*

zavargo@ic.uma.es

[2] *Institute of Photonics and Electronics AS CR, v.v.i., Chaberska 57, 18251 Prague, Czech Republic*

In order to improve accuracy and efficiency of numerical simulations of bent waveguides and ring microresonators we implemented the conformal transformation of coordinates into the Fourier modal method based on fast Fourier transformation. Principles of the method and some examples will be presented.

Introduction

Integrated photonic circuits (IPC) are commonly used in photonic signal processing. For simulation and design of high-contrast devices in which back-reflections have to be properly taken into account, Fourier modal methods (FMM) [1, 2] are often used since they possess both numerical efficiency and good physical insight simultaneously.

Method

In order to improve accuracy and efficiency of numerical simulations of bent waveguides and ring microresonators we implemented the conformal transformation of coordinates [3] into the Fourier modal method for the first time. This conformal transformation helps define a new computational domain in which the circularly bent waveguide is transformed into a rectangle. Then, "standard" FMM with perfectly matched layer (PML) absorbent boundary conditions is used to simulate wave propagation and attenuation. This approach is especially advantageous for the simulation of bent segmented and/or subwavelength grating waveguide structures.

Results

The method has been implemented to validate this proposal. We compared [Figure 1.a)] the propagation constants and radiation losses of eigenmodes of a curved waveguide obtained using two different approaches: the method proposed here and the commercial simulator "Fimmwave". Results are almost coincident. Figure 1.b) shows the field propagation in the curved waveguide.

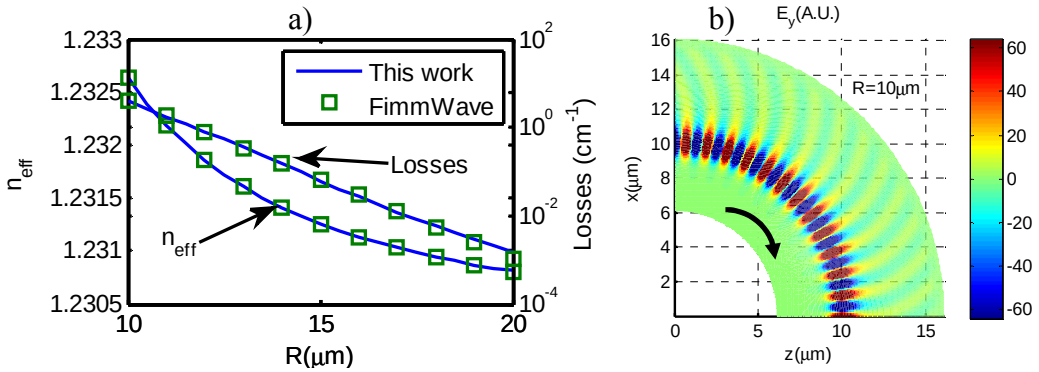

Figure 1. a) Modal effective index and losses of a curved waveguide of central radius R. **b)** Real part of the electrical field. Waveguide width: 400nm. Core refractive index: 1.5. Cladding refractive index: 1. Light wavelength: 1.55μm.

References

[1] L. Zavargo-Peche, et al., *Progress in Electromagnetic Research*, **123**, 447-465, (2012).

[2] J. P. Hugonin, et al., *Opt. and Quantum Electron.*, **37**, 107-119, (2005).

[3] M. Heiblum, et al., *IEEE J. of Quantum Electron.*, **QE-11**, 75-83, (1975).

3D photonic structure modeling with efficient Fourier modal methods

Pavel Kwiecien[1], Ivan Richter[1], and Jiří Čtyroký[2]

[1] *Czech Technical University in Prague, Faculty of Nuclear Sciences and Physical Engineering*
Department of Physical Electronics, Břehová 7, 11519 Prague 1, Czech Republic
pavel.kwiecien@fjfi.cvut.cz, ivan.richter@fjfi.cvut.cz

[2] *Institute of Photonics and Electronics AS CR, v.v.i., Chaberská 57, 182 51 Praha 8, Czech Republic*
ctyroky@ufe.cz

Three dimensional (3D) aperiodic rigorous coupled wave analysis (aRCWA) technique, together with the 3D bi-directional mode expansion and propagation method (BEX3), have been developed and applied as the efficient and robust frequency-domain simulation tools for modeling both modal and propagation characteristics of 3D subwavelength waveguiding and / or plasmonic nanostructures.

Introduction

Today, as subwavelength-structured photonic and/or plasmonic nanostructures are emerging as a class of very promising and versatile structures for various applications, in devices such as filters, switches, modulators, sensors, or lasers, in both passive and active regimes, there is a need for new theoretical exploitations of numerical methods and modeling activities in connection towards their direct application to realistic 3D geometries and problems. We have developed (FNSPE) the efficient 3D aperiodic Fourier modal method (aRCWA) [1], based on the 2D periodic grating algorithm RCWA, using the expansion of field and permittivity and permeability components into complex exponentials. A similar method (denoted as BEX3) has been developed at IPE, too, based on the 2D approach developed earlier. It differs from aRCWA mainly in the application of trigonometric *sin* and *cos* functions instead of complex exponentials. Complex transformations of both transversal coordinates are used as PML in both methods, aRCWA is also equipped with adaptive spatial resolution algorithm [2], and utilization of structural symmetries.

Results

Recently, we have applied our in-house 3D aRCWA method to number of challenging simulation problems, including a novel type of segmented subwavelength-grating (SWG) waveguide ([3,4], see Fig), proposed recently, various plasmonic nanostructures (e.g. COST MP0803 modeling task of long-range plasmonic waveguide, dielectric-loaded surface plasmon-polariton (SPP) waveguide [5]), as well as recent COST MP0702 modeling task of high *Q* photonic crystal nanocavities [6]. Further, a comparison of our two methods, together with several other examples and their mutual comparison will be discussed.

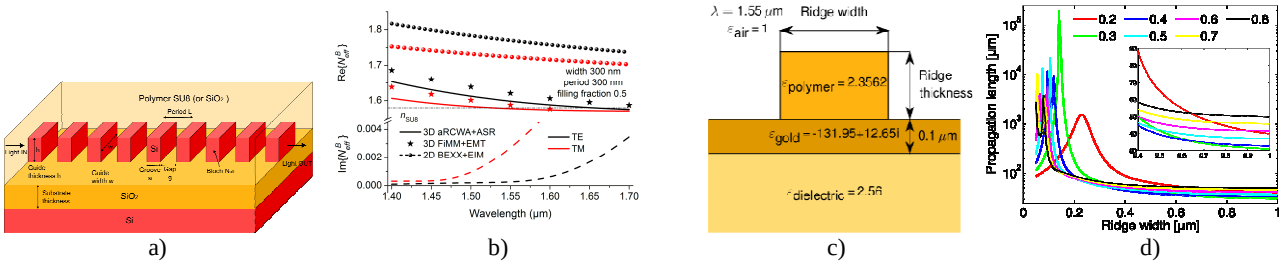

a) b) c) d)

Fig. a) Schematic picture of segmented SWG waveguide, b) effective refractive indices of quasi-TE and quasi-TM Bloch modes with respect to operating wavelength, c) schematic picture of dielectric-loaded SPP waveguide, and d) the propagation length as a function of ridge width of this DLSPP structure.

Acknowledgements: This work was financially supported by the Czech Science Foundation (projects P205/10/0046 and P205/12/G118) and by the Ministry of Education, Youth and Sports of the CR (projects OC09038 and OC09061).

References

[1] E. Silberstein, P. Lalanne, J.P. Hugonin, and Q. Cao, J. Opt. Soc. Am. A, **18**, 2865-2875 (2001).
[2] J. Čtyroký, P. Kwiecien, I. Richter, *J. Lightwave Technol.*, **28**, 2969-2976, (2010).
[3] P. Cheben, P. J. Bock, J. H. Schmid, et al., *Optics Letters*, **35**, 2526-2528 (2010).
[4] J. Čtyroký, I. Richter, P. Kwiecien, *Proceedings of SPIE*, **8306**, 83060Y (2011).
[5] P. Kwiecien, I. Richter, paper JWA41, *FiO OSA Annual Meeting* (October 2011, San Jose, USA, 2011).
[6] J. Petráček, J. Luksch, B. Maes, S. Burger, P. Kwiecien, I. Richter, *MINAP - Micro- and nano-photonic materials and devices* (January 2012, Trento, Italy, 2012).

Simulation of 3D Photonic Nanostructures Using a Bidirectional Eigenmode Propagation Algorithm

Jaroslav Luksch and Jiří Petráček
Institute of Physical Engineering, Brno University of Technology, Technická 2, 616 69 Brno, Czech Republic
petracek@fme.vutbr.cz

We present a new implementation of a bidirectional eigenmode propagation algorithm for simulation of 3D waveguide structures. The eigenmodes are searched using a finite-difference or finite-element modesolver. The technique is applied to the modeling of high-*Q* nanocavity with 1D photonic gap.

Introduction

Simulation of photonic nanostructures is of fundamental importance in the analysis and design of new devices. Among various computational techniques, the modal methods, such as the bidirectional eigenmode propagation [1] (BEP, also known as the mode matching method), have been proven to provide reliable results without excessive demand for hardware resources. A key part of any modal technique is a fast and reliable routine for finding of sufficiently large number of eigenmodes. That is why the techniques have been mainly used for simulation of structures with analytical modal solutions (e.g. 2D devices composed of 1D multilayer waveguides). Recently, the full-vector BEP technique for 3D structures has been developed [2]; eigenmodes have been calculated using the finite-difference technique. The aim of this work is to extend this approach and present our own research on a 3D BEP.

Results

We use two different full-vector techniques for calculating of eigenmodes: a finite-difference (FD) modesolver WGMODES [3] and a finite-element (FE) technique implemented within the COMSOL Multiphysics environment. The propagation technique follows the standard formulation, see e.g. [2,4]. Note, that the algorithm employs numerically stable scattering matrices, which are determined from overlap integrals of modal fields. We will present convergence properties and compare various ways for obtaining the scattering matrices. In particular, we will discuss a non-orthogonality error, which arises as a consequence of discrete representation of the modal fields.
To demonstrate the technique we will present simulation of a numerically challenging structure, high-*Q* nanocavity with 1D photonic gap. The structure, which was inspired with [5], consists of a size-modulated 1D stack cavity coupled with the waveguide. Results indicate that the developed technique is able to provide important characteristics of 3D devices with relatively small effort.

Acknowledgments

This work was supported by the Czech Science Foundation under contract P205/10/0046.

References

[1] G. Sztefka and H.-P. Nolting, *IEEE Photon. Technol. Letters*, **5**, 554-557, (1993).

[2] J. Mu and W.-P. Huang, *Opt. Express*, **16**, 18152-18163, (2008).

[3] A. B. Fallahkhair, et al., *J. Lightwave Technol.*, **26**, 1423-1431 (2008).
www.photonics.umd.edu/software/wgmodes

[4] P. Bienstman and R. Baets, *Opt. Quantum Electron.*, **33**, 327-341, (2001).

[5] M. Notomi, et al. *Opt. Express*, **16**, 11095–11102, (2008).

Novel Silicon Wire Waveguide Crossing with Negligible Loss and Crosstalk

Andrey V. Tsarev
Laboratory of Optical Materials and Structures, A.V. Rzhanov Institute of SB RAS, Novosibirsk, 630090, Russia
tsarev@isp.nsc.ru

Introduction

Efficient silicon wire waveguide crossing by means of vertical coupling of tapered Si wire with upper SU-8 polymer wide strip waveguide through a silica buffer had been studied by 3D FDTD. It provides 98% and 99.9% efficiency for through and cross pass, respectively, and cross talk -70 dB.
Results
The proposed structure of adiabatic three layer cross coupler [1] contains two Si wire waveguide with two contra directed inverse tapers on buried oxide (BOX) silicon substrate which are separated by small distance L_g =3 μm from the taper ends (see Fig.1). The spacing between waveguides contains similar Si wire intersecting waveguide in cross direction (X). The tapered waveguides are covered through spin-on flowable oxide (FOX) buffer and by upper single mode SU-8 polymer strip waveguide (with refractive index N_w=1.56) which is situated just under through pass Si wire (along Z) at distance W_g from it. We examine and optimize by 3D FDTD the power transmittance from one to another Si wire waveguides. Result of typical 3D finite difference time domain (FDTD) simulation is presented on Fig.1 [1]. It shows that by means of Si wire tapers the optical power coupled up and down into the upper polymer waveguide, and thus passes over the crossed Si wire waveguide. It provides negligible power reflection (-50 dB) and scattering into crossing waveguide (-70 dB) as well as negligible loss for through pass (<0.1 dB) and cross pass (<0.002 dB).
The author thanks RSoft Design Group, Inc. for providing software for FDTD simulations.

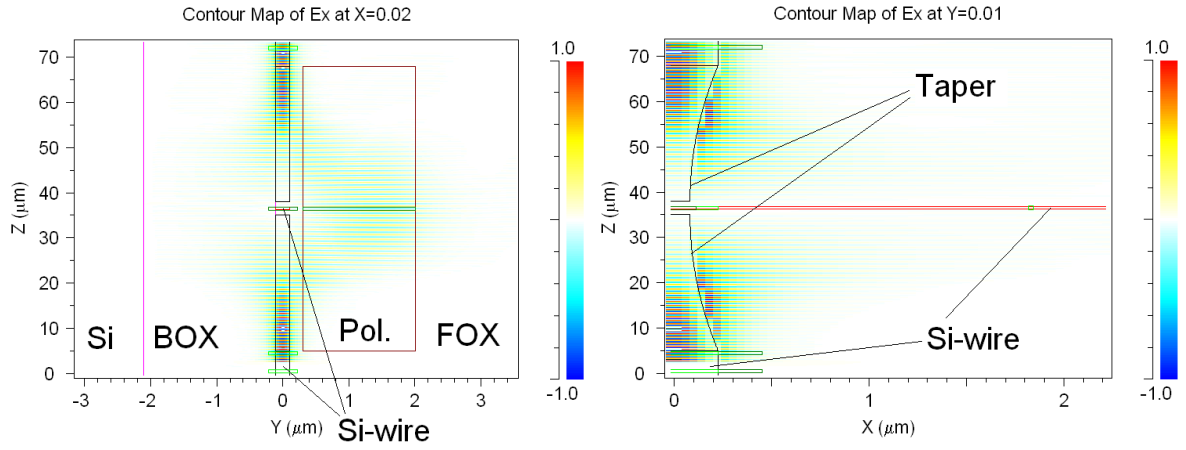

a) b)

Fig.1. Counter map of power transmittance through adiabatic three layer cross coupler of fundamental guided mode of Si wire waveguide. a) X-cut, b) Y-cut (due to symmetry we use half structure, X ≥ 0). Spacing between tips L_g =3 μm, Polymer waveguide (Pol.) width W = 1.5 μm and height H = 1.7 μm, FOX buffer height W_g = 200 nm, parabolic taper length L = 30 μm and tip d = 16 nm, Si wire waveguide width w = 450 nm and height h = 220 nm. 3D FDTD simulation.

References

[1] Andrei V. Tsarev, Opt. Express, **19**, 13732-13737, (2011).

A New TLM Model for Thin Optical Features

Xuesong Meng, Phillip Sewell, Ana Vukovic, and Trevor M. Benson
George Green Institute for Electromagnetics Research, Faculty of Engineering, University of Nottingham, University Park, Nottingham, NG7 2RD, UK
eexxm2@nottingham.ac.uk

In this paper, a new model for thin optical features based on the Transmission Line Modeling (TLM) method [1] is introduced. The fine features are embedded between TLM nodes without discretization. For illustrative purposes this model is applied to calculate the reflection coefficient of a quarter-wavelength antireflection coating (AR).

Introduction

The Transmission Line Modeling (TLM) method [1] is a full wave numerical simulation method. It usually involves discretizing the materials. For very thin optical features, a fine mesh is thus needed, which results in longer run time and larger memory storage. Therefore, a new model embedding thin slabs between TLM nodes, without discretization, is presented.

In this model, a one-dimensional (1D) thin slab is embedded between two TLM nodes as a section of transmission line. The implementation of this new 1D model starts with the admittance matrix of the material. Known analytical expansions for cotangent and cosecant functions in the admittance matrix are introduced to get the formulations in the frequency domain. Then an inverse Z transform and digital filter theory are utilized to transfer the formulations to the time domain. Finally, a Fast Fourier Transform (FFT) is taken to get the reflection coefficients of the slab.

Results

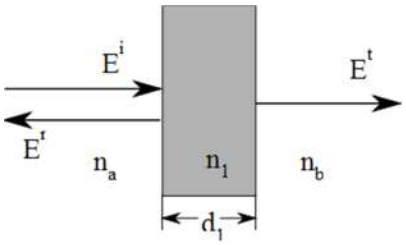

Fig.1 The electric field is normal incident to a quarter-wave slab on a glass substrate. $n_a = 1, n_1 = 1.22, n_b = 1.5, d_1 = 112.71nm$

By way of illustration the model is used to calculate the reflection coefficients of a quarter-wavelength antireflection coating (AR). This AR coating [2] has a refractive index of 1.22 on a glass substrate with index 1.5, and is a quarter-wavelength thick at $\lambda_0 = 550nm$, that is $d_1 = \frac{\lambda_0}{4n_1} = 112.71nm$. As in Fig.1, the electric field is normally incident from free space (n_a) on to the slab (n_1) and then emerges into the glass substrate (n_b). Fig.2 shows the reflection coefficients results obtained from our model with different orders of the expansions used to approximate the cotangent and cosecant functions. These results are compared to the analytical ones obtained from a transfer matrix approach. The TLM results show indistinguishable agreement with the analytical ones when higher expansion orders are used.

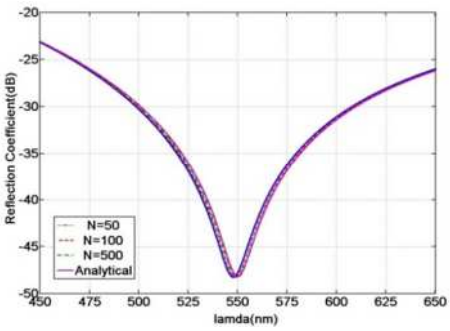

Fig.2 The reflection coefficients of the quarter-wave slab. N is the order of the expansions approximate to the cotangent and cosecant

Reference

[1] C. Christopoulos, IEEE press, New York (1995)

[2] S. J. Orfanidis, *on-line book*, available: www.ece.rutgers.edu/~orfanidi/ewa.(2010)

Propagation of a Gaussian Pulse in a Coaxial Optical fiber: effect of two mode interference

Enakshi K Sharma[1], Jyoti Anand[2], and Jagneet Kaur Anand[2]
[1] *Department of Electronic Science, University of Delhi South Campus, Delhi-110021, India*
enakshi54@yahoo.co.in
[2] *Keshav Mahavidyalaya, University of Delhi, Delhi 110034, India*

We show that a Gaussian temporal light pulse propagating through a coaxial fiber splits into a series of narrow pulses within the broadened Gaussian envelope due to the interference between the two excited supermodes, which have equal and opposite group velocity dispersion(GVD) at a chosen wavelength.

Summary

Coaxial fibers (Fig.1) have been widely studied as dispersion compensating fibers considering only the propagation of the LP_{01} supermode with negative dispersion [1,2]. However, we note that the coaxial fiber supports both the LP_{01} and LP_{02} supermodes which at a certain wavelength,λ_o, have the same group velocity, v_o (Fig.2) and almost equal and opposite group velocity dispersion.

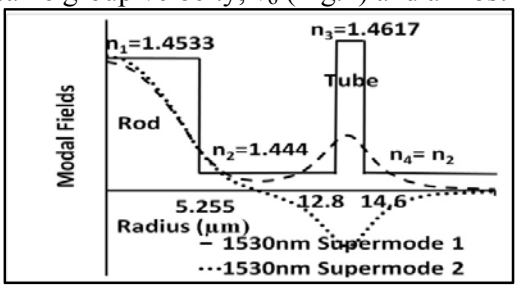

Fig. 1 Index profile and supermodes of the coaxial fiber

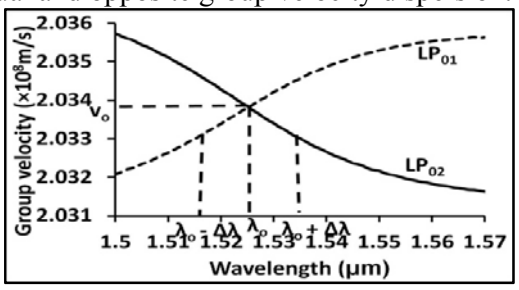

Fig. 2 Group velocity of two supermodes vs λ

When the coaxial fiber is excited by Gaussian temporal pulse of the form $E = E_o \exp(-\frac{t^2}{\tau_o^2})\exp(j\omega_o t)$ with $\omega_o = \frac{2\pi c}{\lambda_o}$ and spectral spread ~2.5nm ($\tau_o = 1ps$), from a single mode fiber identical to the rod waveguide of the coaxial fiber, both supermodes are almost equally excited [3]. Due to opposite GVD both supermodes have the same group delay for wavelengths $\lambda_o \pm \Delta\lambda$ (Fig. 2) and hence arrive at a distance, z, at the same time. Due to interference between the supermodes, the light coupled into an output single mode fiber consists of a series of narrow pulses within the broadened Gaussian envelope (Fig. 3). No significant frequency chirping is seen across the envelope.

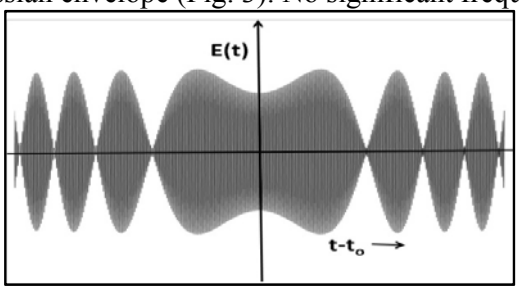

Fig. 3a Field variation of output pulse with time

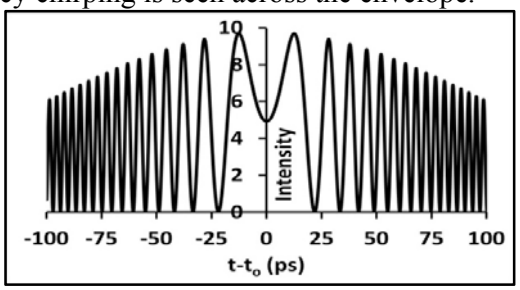

Fig. 3b Intensity of output pulse at z~400m; $t_o=z/v_o$

References

[1] **A.** Joseph Antos and David K. Smith, *J. Lightwave Technol.*, **12**, 1739-1745, (1994).

[2] K. Thyagarajan, et al., *IEEE Photon. Technol. Lett.*, **8**, 1510-1512, (1996).

[3] Jyoti Anand, et al., *Optics & Laser Tech.*, **45**, 688-695, (2012).

HCMT interaction of whispering gallery modes in circuits of integrated optical microring or -disk resonators

Ellen F. Franchimon [a], Kirankumar R. Hiremath [b], Remco Stoffer [c], and Manfred Hammer [a]
[a] *MESA+ Institute for Nanotechnology, University of Twente, Enschede, The Netherlands*
[b] *Computational Nano-Optics Group, Zuse Institute, Berlin, Germany*
[c] *PhoeniX Software, Enschede, The Netherlands*
m.hammer@ewi.utwente.nl

Whispering gallery modes (WGMs) supported by open circular dielectric cavities are embedded into a 2-D hybrid coupled mode theory (HCMT) framework. The model enables convenient studies of supermode formation in composite circuits (CROWS, photonic molecules), and of their excitation by straight access channels.

Summary

Whispering gallery modes (WGMs*) of dielectric disks or rings, prototypes for the eigenmodes of open optical cavities, are characterized by by their *complex* eigenfrequency, *integer* angular wavenumber, and, in 2-D, by a radial order. We introduce analytical WGMs into a framework of hybrid analytical / numerical coupled mode theory (HCMT, [1]). The model relies on a plausible "template" for the overall field. Known profiles, typically directional guided modes of optical channels, are superimposed with unknown influence functions. WGMs enter with single coefficients. Upon discretizing any unknown functions by 1-D finite elements, a Galerkin procedure, based on the first order Maxwell equations in the frequency domain, leads to a set of linear algebraic equations. For given input the response for the prescribed frequency is obtained. For a configuration without excitation, looking for nontrivial solutions establishes an eigenvalue problem for the "supermodes" (SMs) of the composite circuit. We benchmark this approach versus bend-mode (*real* frequency and *complex* angular wavenumber) HCMT [2], conventional CMT ([3], couplers only), and FDTD. The WGM-HCMT model permits easily interpretable studies of SM formation in quite arbitrary composite structures, of their perturbation, and of their excitation by straight access channels. Coupling induced shifts of resonance frequencies [4] or similar effects can be investigated conveniently and systematically.

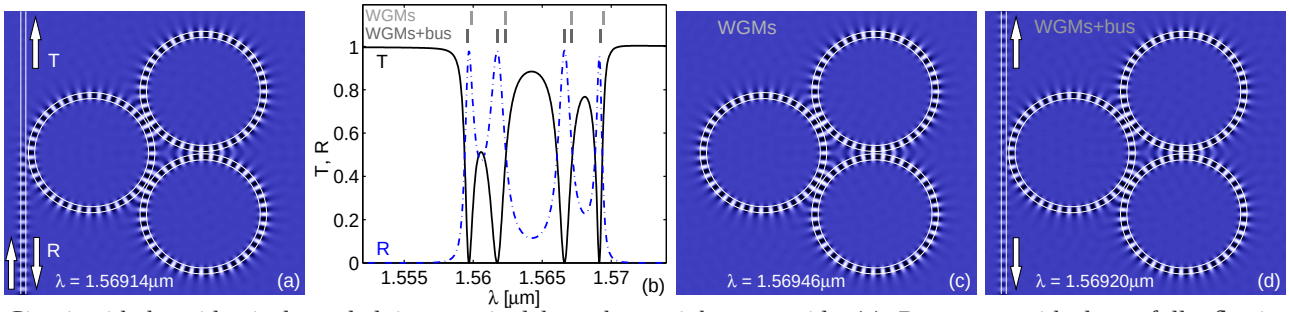

Circuit with three identical coupled rings, excited through a straight waveguide. (a): Resonance with almost full reflection of the incoming wave. (b): Spectral transmission and reflection (WGM-HCMT model) around the WGM$_{(0,\pm 39)}$ resonance at 1.5637 μm of a single ring (free spectral range ≈ 35 nm); vertical lines: SM resonance wavelengths, cavities only (top row), and cavities + bus. (c): "Fundamental" SM of the three-ring "molecule", HCMT model with 6 unknowns based on the directional WGMs of the individual rings. (d) Respective SM of the entire structure, here the HCMT template includes also the vertical modal outlets. 2D-TE simulations; time snapshots of the single electric field component; parameters: refractive indices 1.5, 1.0, ring radii 7.5 μm, core widths 0.75 μm (rings) and 0.6 μm (bus), gaps 0.3 μm.

References

[1] M. Hammer. *Journal of Lightwave Technology*, 25(9):2287–2298, 2007.
[2] M. Hammer. *Journal of the Optical Society of America B*, 27(11):2237–2246, 2010.
[3] K. R. Hiremath, R. Stoffer, and M. Hammer. *Optics Communications*, 257(2):277–297, 2006.
[4] M. A. Popović, C. Manolatou, and M. R. Watts. *Optics Express*, 14(3):1208–1222, 2006.

* For lack of a better name, we apply the term WGM also to cavities with more than one circular interface.

FDTD Simulation of Acousto-Optic Filter with Beam Expanders Constituted by Photonic Crystal Rows of Airholes in $LiNbO_3$ Waveguides

Andrey V. Tsarev
Laboratory of Optical Materials and Structures, A.V. Rzhanov Institute of SB RAS, Novosibirsk, 630090, Russia
tsarev@isp.nsc.ru

Introduction

A new compact AO filter with multi-reflector beam expanders built by photonic crystal row of holes in $LiNbO_3$ waveguide had been numerically studied by 2D FDTD method. Device has the size 70*150 μm^2, FWHW 4.4 nm, tuning range 110 nm, internal loss -3dB, and sidelobes -20 dB.
Results
The typical AO filter design is presented on Fig.1a [1]. Input TE-polarized optical beam path through the channel optical waveguide (8) that is crossed by multiple partial reflectors which are built by the row of holes (7) vertically etched through the total waveguide height. Input beam splits by the partial reflectors into multiple sub-beams of proper designed amplitude and phase, and enter into the slab waveguide region (2) where propagates the surface acoustic wave (SAW) that is launched by interdigital transducer (7). All sub-beams interfere and form the wide optical beam that comes to the area of acoustooptic interaction and diffracted by SAW (5). Diffracted beam tilts with the SAW wavelength according to the Bragg conditions. Second beam expander (9) works as reciprocal elements. It can filter only that optical wavelength which interfere and add in sum along the axis of the beam expander. By changing the SAW frequency (or SAW wavelength Λ) filter can Drop different optical wavelength. Performances of the device in Ti:$LiNbO_3$ waveguide with 32 reflectors had been investigated by 2D finite difference time domain (FDTD) method (see Fig.1b). It is numerically demonstrated that AO filter provides unique line width by AO length product 0.7 μm^2. By extrapolating this result to real devices with hundreds of reflectors [1], one can develop widely tunable AO filters with 0.1 nm linewidth and multi-hundred wavelength channels.
The author thanks RSoft Design Group, Inc. for providing software for FDTD simulations.

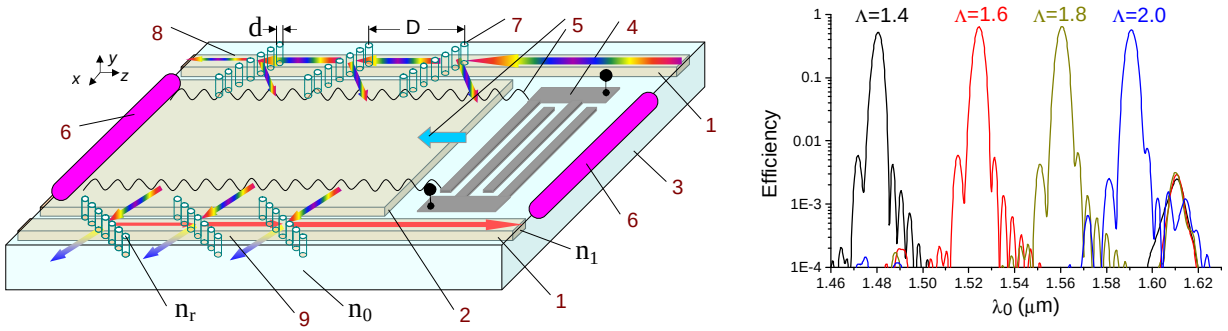

a) b)

Fig.1. Noncollinear AO fillter built by the rows of holes. a) General view; b) AO filter response for the different Λ (in μm). 2D FDTD simulation of structure with variable holes diameter and position. (1) channel waveguide; (2) planar waveguide; (3) piezoelectric substrate; (4) interdigital transducer; (5) SAW; (6) SAW absorber; (7) elementary reflector by row of holes; (8) first beam expander; (9) second beam expander

References

[1] Andrei V. Tsarev, *Opt. Lett.*, **35**, 4033-4035, (2010).

Compact Multi-Splitting Widely Tunable Filter on SOI Technology

Andrey V. Tsarev
Laboratory of Optical Materials and Structures, A.V. Rzhanov Institute of SB RAS, Novosibirsk, 630090, Russia
tsarev@isp.nsc.ru

Introduction

This paper proposes and makes simulation by 2D FDTD of new tunable optical filter which utilized multiple coupled silicon wire waveguides on SOI structures. It provides wavelength tuning (without Vernier principle) within total FSR 36.8 nm at 1.55 μm by temperature increment ΔT< 100 C°.

Results

Novel filter design joint together advantages of multi-reflector (MR) [1] and lattice Mach–Zehnder filter [2] technologies by using the directional couplers for power splitting and MR-like structure design for optical filtering and tuning. Parameters of all waveguides are corresponded to typical silicon wire with 450 nm width and 250 nm height built on silicon-on-insulator (SOI) structure. We utilize the Gaussian apodization function (for providing high sidelobes suppression) by the control of splitting ratio as a function of coupling gap *d*. Light propagation through the filter at Drop wavelength is shown in Fig. 1a. Device can be tuned (see Fig. 1b) within total FSR by changing the temperature in fine tuning and wide tuning phase shifters similar to the case of MR filter [1].
The author thanks RSoft Design Group, Inc. for providing software for FDTD simulations.

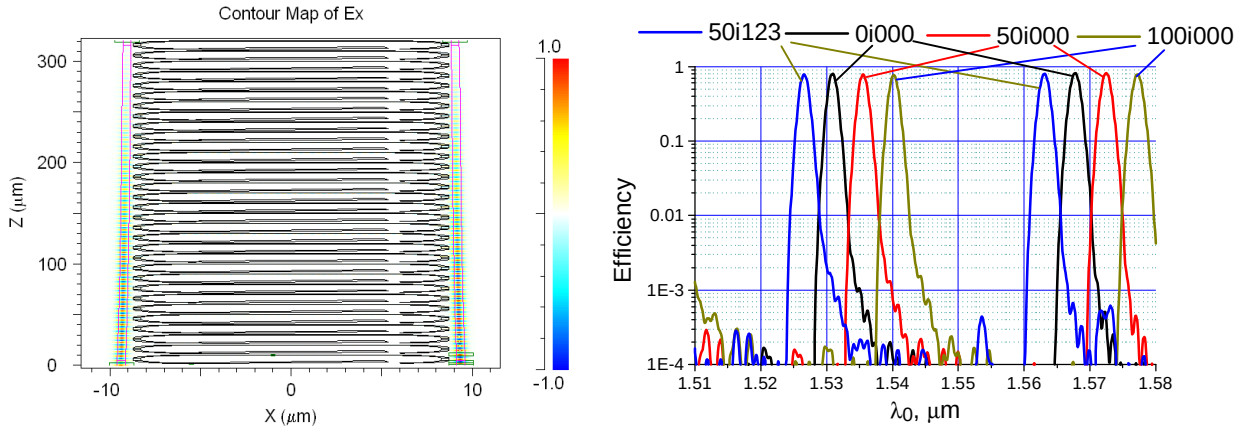

a) b)

Fig.1. Multi-splitting filter. a) Simulated structure; b) Internal efficiency for different temperature increments (*DT* = 0°, 50°, 100°) in fine and wide tuning (with step FSR/4 by *DT00*) phase shifters. Total length *L* = 321 μm, radius *R* = 3 μm, linewidth *Dl* ~ 1.7 nm, FSR ~ 36.8 nm. Notation (*i***) means setting for different temperature *DT* and integer numbers for wide tuning, namely, 50i123 corresponds to the case: *DT* = 50 C°, *DT1* = 1×ΔT00, *DT2* = 2×*DT00*, and *DT3* = 3×*DT00*.

References

[1] F. De Leonardis, A. V. Tsarev, and V. M. N. Passaro, *Opt. Express*, **16**, 21333–21338, (2008).
[2] K. Yamada, T. Shoji, T. Tsuchizawa, T. Watanabe, J. Takahashi, and S. Itabashi, Opt. Lett., **28**, 1663–1664, (2003).

Large, integrated spot size converter for an InGaAs PIN-photodiode

Andreas Wieczorek[1,2], Yang Hua[1], Brendan Roycroft[1], Frank H. Peters[1,2] and Brian Corbett[1]
[1] *Tyndall National Institute, Dyke Parade, Lee Maltings, Cork, Ireland*
andreas.wieczorek@tyndall.ie
[2] *Physics Department, University College Cork, Cork, Ireland*

A high speed photodiode with a $1/e^2$ input mode size of 9 µm using an integrated mode converter is presented. The coupling loss to a standard cleaved single mode fiber is calculated to be 0.1 dB. The absorption efficiency for refractive indices, layer thickness and etch depth variations is simulated.

Introduction

Photodiodes are one of the key components in photonic integrated circuits. However, a mode mismatch between a cleaved fiber and an InGaAs PIN-photodiode (PIN-PD) results in losses of 10 dB or more. The asymmetric twin waveguide (ATG) [1, 2] offers a relatively easy to fabricate approach to improved fiber coupling. Nevertheless, a lensed fiber was required to couple the input signal. Here we show the design of a PIN-PD with an input waveguide with a spot size of 9 µm suitable for polarization insensitive coupling from a cleaved fiber input. The absorption efficiency is simulated relative to the matching layer refractive index/thickness, relative to the quaternary refractive index/thickness and relative to the n-contact etch-depth at the PD.

Results

Fig. 1 shows a schematic diagram of the device. The optical field couples into the diluted waveguide on the left and is transferred in a polarization insensitive manner into the PD via two waveguides. To enable the nearly loss less field transition two tapers are introduced (taper 1: start width: 1 µm, end width: 5 µm, length: 1220 µm; taper 2: start width: 1 µm, end width: 3 µm, length: 350 µm). The absorbance efficiency (AE) of the PD is shown relative to a variation of the refractive index of the matching layer (Fig. 2). The refractive index can only vary by around 0.02 to an optimum value of 3.32 to keep the AE > 90 %.

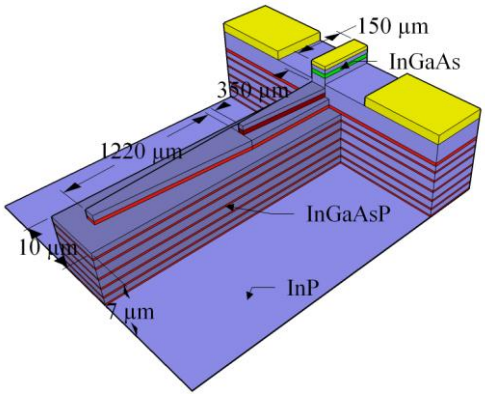

Fig.1: Schematic diagram of the spot size converter and the InGaAs photodiode.

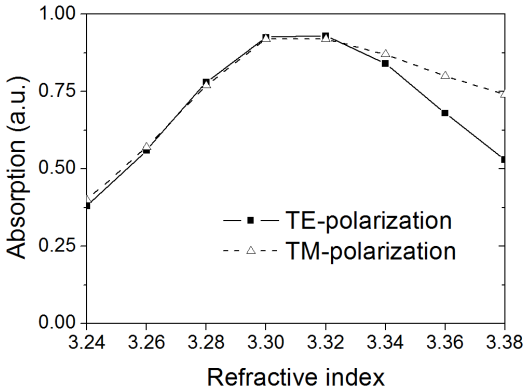

Fig.2: Absorption relative to the refractive index of the matching layer.

References

[1] P.V. Studenkov, et al., *IEEE Photon. Technol. Lett.*, **10**, 1088-1090, (1998)

[2] F. Xia, et al., *IEEE Photon. Technol. Lett.*, **13**, 845-847, (2001)

A factorable photon pair source based on silicon nanowires

S. Khasminskaya[1], H. X. Tang[2] and W. H. P. Pernice[1]
[1] *Karlsruhe Institute of Technology (KIT), Institute of Nanotechnology, Hermann-von-Helmholtz-Platz 1, 76344 Eggenstein-Leopoldshafen, Germany*
[2] *Yale University, Department of Electrical Engineering, 15 Prospect Street, New Haven CT 06511, USA*
wolfram.pernice@kit.edu

Through dispersion engineering of silicon nanowire waveguides we simultaneously achieve group-velocity and phase matching. By exploiting spontaneous four-wave-mixing, two-photon states with reduced spectral correlations can be generated.

Introduction

Nanophotonic waveguides provide tight confinement of light into sub-wavelength structures, which leads to significant field enhancement within the waveguide core. Therefore such structures are ideally suited for non-linear optical applications. Because silicon possesses a high third order nonlinear coefficient compared to silica glass, four-wave mixing (FWM) in nanowire waveguides has been of great interest for integrated nonlinear optical devices [1]. In particular, exploiting spontaneous FWM for the generation of correlated photon pairs provides a viable route for integrated single photon sources.

Here we show that by dispersion engineering silicon waveguides group velocity matching (GVM) in addition to phase-matching required for FWM, can be achieved, providing a route towards factorable photon states on chip.

Results

The dispersion properties of silicon ridge waveguides atop a buried oxide layer (as shown in Fig.1a)) can be tuned by varying the waveguide width *w*. As a result of anomalous geometric dispersion offsetting the intrinsic normal chromatic dispersion of silicon, phase-matching in the telecoms band around 1550nm can occur (black line in Fig.1b)). When simultaneously the waveguide height is adjusted GVM along the light blue line in Fig.1b) is achieved. Here the color coded background indicates the phase matching angle (PMA) as defined in [2]. In Fig.1b) the light blue lines indicate the GVM contours with a PMA of 45 degrees. At the points where the GVM curve intersects with the phase-matched curve, factorable photon states can be generated. The corresponding wavelengths of the signal and idler photons can further be tuned by varying the power of the input pump light. The resulting possibility of achieving factorable states on a chip thus alleviates the stringent requirements on photonic filter circuitry needed for heralding single photons.

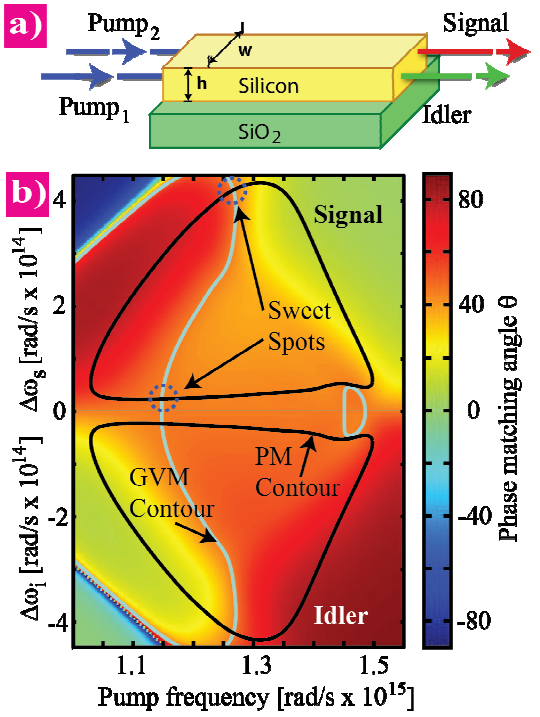

Fig.1 a) Parameters of the ridge waveguide used for FWM. b) The color coded calculated PMA. Overlaid are the contours for PM (black line) and GVM (blue line).

References

[1] M.A. Foster, et al.,*Nature* **441**, 960-3, (2006).
[2] K. Garay-Palmett, et al., *Opt. Express* **15**, 14870-14886 (2007).

Three-dimensional FFT-based generalized rectangular wide-angle beam propagation method with complex Jacobi iteration

Rafael Godoy-Rubio, and Alejandro Ortega-Moñux
Dpto. Ingeniería de Comunicaciones, Universidad de Málaga, Campus Teatinos s/n, 29071, Málaga, Spain
faligr@ic.uma.es

In this work we propose a new three-dimensional FFT-based wide-angle beam propagation method (WA-BPM) using a generalized envelope function and incorporating complex Jacobi iterative (CJI) schemes. The inclusion of FFT-based strategies preserves the computational efficiency in 3D scenarios. Besides, the CJI algorithm's convergence rate, as in previous Fourier-based implementations, is improved with respect to the original space domain version.

Introduction

Recently, a new 2D WA-BPM with complex Jacobi iteration in the Fourier domain has been proposed to analyze nonlinear devices [1]. For certain problems, this Fourier-based implementation has been proven to converge, assuring the same accuracy, at a higher rate than those similar methods based on finite-difference schemes. However, although typical errors from the approximation of partial derivatives can be minimized with Fourier-based strategies, others related to the preferred direction of propagation persist. This drawback was solved in finite difference methods using a generalized rectangular (GR) WA-BPM, achieving an important improvement in the accuracy obtained even with low order Padé approximations and coarse grids [2]. This GR formulation has been extended later to include modified Padé approximants and complex Jacobi iteration as longitudinal solving method, increasing the execution speed considerably [3].
In this work, we try to combine the advantages of both Fourier-based and generalized rectangular formulations in a new WA-BPM. Although the 2D version of the proposed new method implies such relatively low effort, its extension to three dimensions leads to deep changes in order to keep its computational efficiency. These changes result in a version of the generalized rectangular WA-BPM which incorporates complex Jacobi iteration to solve the problem in the longitudinal direction and FFT-based strategies to perform transverse discretization [4].
The resultant FFT-based CJI-GR-WA-BPM has been validated in 2D and 3D situations. When compared to the original finite difference approach, FFT-based method shows a higher convergence rate, confirming the conclusions exposed in [1]. Furthermore, thanks to the FFT-based approach, its computational efficiency is preserved even for 3D problems requiring a high number of Fourier coefficients.

References

[1] R. Godoy-Rubio, et al. *J. Opt. Soc. Am. B*, **28**, 2142-2148, (2011).

[2] S. Sujecki. *Appl. Opt*., **25**, 138-145, (2008).

[3] Khai Q. Le, et al. *J. Opt. Soc. Am. B*, **26**, 1469-1472, (2009).

[4] A. Ortega-Moñux, et al. *IEEE Photon.Technol. Lett*. **19**, 414–416, (2007).

Nonlinear Surface Wave Peculiarities in the Metal Covered SBN:75 Photorefractive Crystal

Jamil Nurligareev, Boris Usievich, Vladimir Sychugov, Liudmila Ivleva
General Physics Institute, Vavilov street 38, 119991, Moscow Russia
borisu@kapella.gpi.ru

Influence of the adjacent medium on the light propagation close to the boundary of photorefractive crystal is studied.

Introduction

Nonlinear surface waves in photorefractive crystals (PR SW) [1] are under investigation during the latest years. The most attractive feature of PR SW is that the concentration of beam energy in the narrow surface layer significantly increases the operation speed of the photorefractive devices without the need for prefabricated waveguiding structures. A very strong enhancement of all nonlinear surface optical phenomena, such as surface absorbed molecular luminescence, Raman scattering, surface second harmonic generation (SHG). etc. may be expected due to PR SW excitation. SBN crystals are of particular importance due to high values of their electrooptical coefficients [2].

Results

In this paper we analyze the peculiarities of PR SW excitation in the SBN:75 crystal. Studying the near- and far-field of light exiting from the photorefractive crystal illuminated by a grazing focused beam of He-Cd laser with an extraordinary polarization was carried out and allowed us to draw a conclusion that the material characteristics of the adjacent medium can affect significantly the photo-induced scattering and the profile of the resulting surface wave.
Using method of images [3] we modelled the distribution of the electrostatic field formed by a Gaussian light beam (wavelength 0.44 μm) illuminating the photorefractive crystal close to its boundary with the linear dielectric or metal.
The obtained results allow us to propose the mechanism of nonlinear surface wave formation with the aperiodic distribution of intensity in photorefractive crystals covered by metal.

Acknowledgements

This work was supported by Russian Foundation for Basic Research (grant N10-02-01389) and Federal Targeted Programme “Research and Development in priority development areas of scientific and technological complex of Russia in 2007-2013” (contract N 16.513.12.3019).

References

[1] G.S. Garcia Quirino, et al., Phys. Rev. A., **51**, 1571-1577, (1995)

[2] B A Usievich, et al., Quantum Electron, **41**, 262–266, (2011)

[3] I.E. Tamm, Fundamentals of the Theory of Electricity, Chapter 2, Mir Publishers, (1979)

Transformation of Whispering Gallery Waves in a Spherical Resonator Caused by Permittivity Time Changing

N. Sakhnenko[1], A. Nerukh[1], T. Remayeva[1] and T. Benson[2]
[1] *Kharkov National University of Radio Electronics, Lenin Ave 14, 61166 Kharkov, Ukraine*
nerukh@gmail.com
[2] *George Green Institute for Electromagnetics Research, University of Nottingham, University Park, Nottingham, NG7 2RD, UK*

Evolution of whispering gallery waves in a dielectric spherical resonator with a time jump of refractive index is investigated theoretically. It is shown that transformation of a wave frequency depends on a magnitude of a refractive index jump as well as on an overlap coefficient of a non-stationarity region and a WGW region.

Introduction

Micro- and nano-dimensional optical resonators are very important for a variety of scientific and engineering applications including low-threshold lasers, ultra-small filters, sensors and others [1, 2]. The simplest 3D optical resonator has a form of a sphere. In the vicinity of a curved surface of a spherical resonator whispering gallery waves can be excited due to total internal reflection of the light. Q-factor of these oscillations is extremely high because light becomes trapped within the resonator.

Dynamic resonators and photonic systems in which material parameters can be varied by external forces have great opportunities for their use in all-optical switchers and tunable filters and represent a powerful approach for all-optical control of light [3, 4]. In practice, the temporal switching of the material refractive index can be realized by varying the input signal in a nonlinear structure; by voltage control; by a focused laser beam as a local heat source or else by free carrier plasma injection. Typically the value of change in refractive index attainable with present day technology is of the order 10^{-4} .

Results

A 3D problem of transformation of whispering gallery waves in a spherical resonator caused by a time jump of refractive index is investigated theoretically in this paper. A rigorous theoretical method which reduces the Maxwell equations to a Volterra integral equation for vectors of an electromagnetic field in time domain is used.

It is shown that a frequency changes in an opposite direction with respect to changing of a refractive index. Comparison of a frequency shift for waves with different spatial distribution shows the greater shift for modes with greater polar index *n*. Increase of *n* leads to increasing of a Q-factor for oscillations. It means that an electromagnetic field is localized greatly inside the resonator, so the greater an overlap coefficient of a non-stationarity region and a whispering gallerry wave region the greater a frequency shift. It is shown also that the frequency shift for TM modes is greater in comparison with TE modes. It is caused by greater localization of TM modes inside the resonator (in the figure: (a) for TE, (b-c) for TM modes).

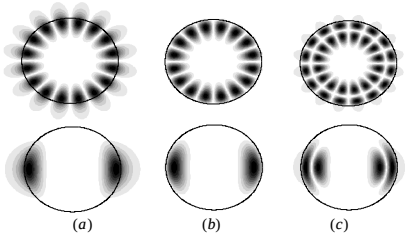

References

[1] K. Vahala. Optical Microcavities, *Nature*, **424**. 839-846, (2003)
[2] A. Savchenkov et al, *IEEE Photonics Technology Letters,* **17**, 136-138, (2005)
[3] A. Liu, R. et al, *Nature* **427**, 615-618 (2004).
[3] N. Sakhnenko, A. Nerukh, J. of Optical Society of America A, **29**, 99-104, 2012.

Waveguide laser modelling of Erbium/Ytterbium activated monoclinic double tungstates

J. Martínez de Mendibil[(1)], G. Lifante[(1)], C. Berrospe [(2)], W. Bolaños[(2)], J.J Carvajal[(2)], M. Aguiló[(2)], F. Díaz[(2)], E. Cantelar[(1)]

[1] *Departamento de Física de Materiales, C-04. Facultad de Ciencias, Universidad Autónoma de Madrid. 28049-Madrid (Spain)*

jon.martinez@uam.es

[2] *Física i Cristal·lografía de Materials i Nanomaterials (FiCMA-FiCNA), Universitat Rovira i Virgili (URV), Campus Sescelades, C/ Marcel·lí Domingo s/n 43007 Tarragona (Spain)*

Introduction

The following paper describes the modelling of Er:Yb:$KY_{1-x-y}Gd_xLu_y(WO_4)_2/KY(WO_4)_2$ ridge waveguides. BPM is used to obtain the modal intensity profiles for pump and emission wavelengths, while overlapping integral method [1,2] is used to determinate the optimum parameters for laser action in this system.

Results

Active KYW waveguides have been successfully developed combining Liquid Phase Epitaxy techniques with micro-structuration techniques such as RIE (*Reactive Ion Etching*) or Ar milling [3]. Using the overlapping integral method, rib waveguide lasers of monoclinic potassium double tungstate, $KRE(WO_4)_2$, co-doped with Erbium and Ytterbium have been modelled. The laser operation at 1.5 μm is based on an efficient pump scheme via the energy transfer from Yb to Er ions. The numerical simulation requires spectroscopic parameters associated to the active ions, waveguide geometry and index profiles, which have been experimentally obtained.

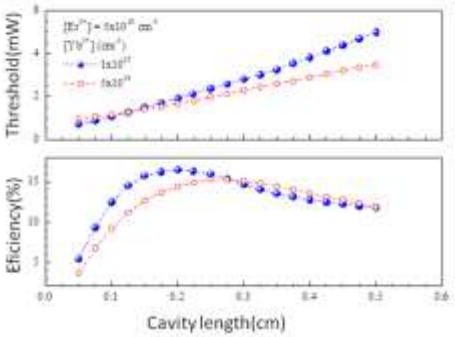

Calculated efficiency and threshold as function of the cavity length.

This model allows determining the laser power as a function of controllable parameters such as ions doping level, pump power, cavity length and reflectance of the input/output mirrors. It has been found that, for the standard doping level used in this matrix, the optimum cavity length is only few millimetres. Overall, using simulation tools is possible to optimize fabrication parameters, and thus saving effort in the development of experimental prototypes.

References

[1] J.A. Vallés, J.A. Lázaro, M.A. Rebolledo, *IEEE J. Quantum Electron.* **32**, 1685-1694 (1996).

[2] E. Cantelar, G. Lifante, F. Cussó, *Opt. Quantum Electron.* **38**, 111-122 (2006).

[3] W. Bolaños, J.J. Carvajal, X. Mateos, G.S. Murugan, A.Z. Subramanian, J.S. Wilkinson, E. Cantelar, D. Jaque, G. Lifante, M. Aguiló, F. Díaz, *Opt. Express* **18**, 26937-26945 (2010).

Impact of Hosting Media on the Specific Resonances of Periodic Grating Embedded in Dielectric Slab

Volodymyr Byelobrov[1], Trevor Benson[2], and Alexander Nosich[1]
[1] *Institute of Radiophysics and Electronics NAS of Ukraine, Proskury st.12, 61085 Kharkiv, Ukraine*
volodia.byelobrov@gmail.com
[2] *George Green Institute for Electromagnetics Research, University of Nottingham, Nottingham, NG7 2RD, United Kingdom*

Introduction

A periodic grating of circular dielectric cylinders in free space possesses specific resonances that have very interesting features [1]. An "active" model of such a grating in a dielectric slab is developed to enable the impact of the host medium on the grating resonances to be studied.

Results

An "active" model for open dielectric resonators is considered, meaning that a region with strictly negative imaginary part of the refractive index or lasing threshold γ, is proposed to compensate the losses for illumination. This value is set at the stage of problem formulation and is sought in tandem with the lasing frequency as solution of a determinant equation for particular structure derived from Helmholtz equation. Smaller threshold values are advantageous and so we are interesting in optimizating this parameter. A grating of circular dielectric cylinders in free space has specific resonances, aligned to its period. They form a multiplex of eigenmodes near the branch point (where the wavelength equals the period); each of the modes tends to this singularity and vanishes there for a large value of the ratio of period to cylinders' radius. However before it disappears, it shows a huge efficiency: in the scattering problem it has a very narrow resonance and in the associated eigenproblem, it gives rise to a small threshold. Fabrication and use of the grating requires its embedding in a dielectric slab of different refractive index. Such slab with embedded grating was investigated using similar approach to [2], the resulting matrix obeys the Fredholm condition that guarantees convergence and is critical for the eigenproblem. The reflectance of a normally incident plane wave on the slab is shown in Fig. 1 (a). Here there are the modes of the slab on the background and six sharp grating resonances. The eigen-problem is conducted by adding an imaginary part to the grating refractive index $\nu = 2 - i\gamma$. The lasing frequencies of the associated eigenmodes, Fig. 1(b), exactly follow the traces of the ones in Fig.1(a). However their lasing thresholds Fig. 1(c) are influenced by the slab modes; in the intersecting areas thresholds decay.

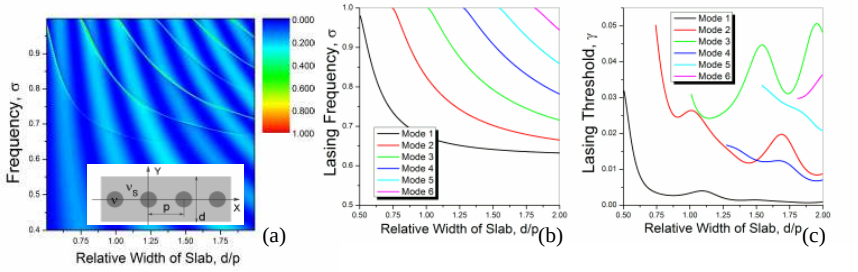

Fig.1 Relief of reflectance in the H-polarization depending on relative slab width and normalized by period frequency. Refractive indexes of slab is $\nu_S = 1.6$ and grating $\nu = 2$ (a). Eigenvalues for corresponding active resonator: lasing frequency (b) and lasing threshold (c).

References

[1] V. Byelobrov *et al. Optics Letters* , **35**, No 21, 3634-3636, (2010)

[2] H. Jia, *et al., IEEE Trans. Antennas Propag.*, **53**, No 3 1145-1152, (2005)

Analysis of 2D Photonic Bandgap Waveguides using a Simple Analytical Method

Kanchan Gehlot and Anurag Sharma
Department of Physics, Indian Institute of Technology Delhi, New Delhi – 110 016, India
gehlot.kanchan@gmail.com, asharma@physics.iitd.ac.in

An analytical approximate method has been tested on two-dimensional photonic bandgap waveguide to study reflection and transmission characteristics. Results show good agreement with available FDTD results.

Introduction

In an earlier work [1], we had shown that the optimal variational (V_{OPT}) method [2] can be adapted with good success to obtain reflection and transmission through photonic crystal slab waveguides. In this paper, we further develop the procedure for 2D photonic bandgap(2D PBG) waveguides.

Results

Variational optimization method, V_{OPT} [2] is used to reduce a 2D PBG waveguide into a 1-D Bragg reflector which is then used to obtain the reflection and transmission characteristics of the waveguide including the photonic bandgap regions [1]. The main structure used in this analysis is a PBG waveguide with a single-mode slab waveguide at the input end (Fig. 1) [3]. To apply V_{OPT} method, the structure has been modified by replacing circular holes by square holes of same area. Transmission coefficient of PBG structure has been computed from converged solution of V_{OPT} iterations for incident fundamental TE mode of slab waveguide. This result is plotted along with FDTD results taken from ref. [3]. The results show good agreement; the deviations in the reflection results are due to some losses, which show up in the FDTD results [3]. Further work to incorporate losses is in progress.

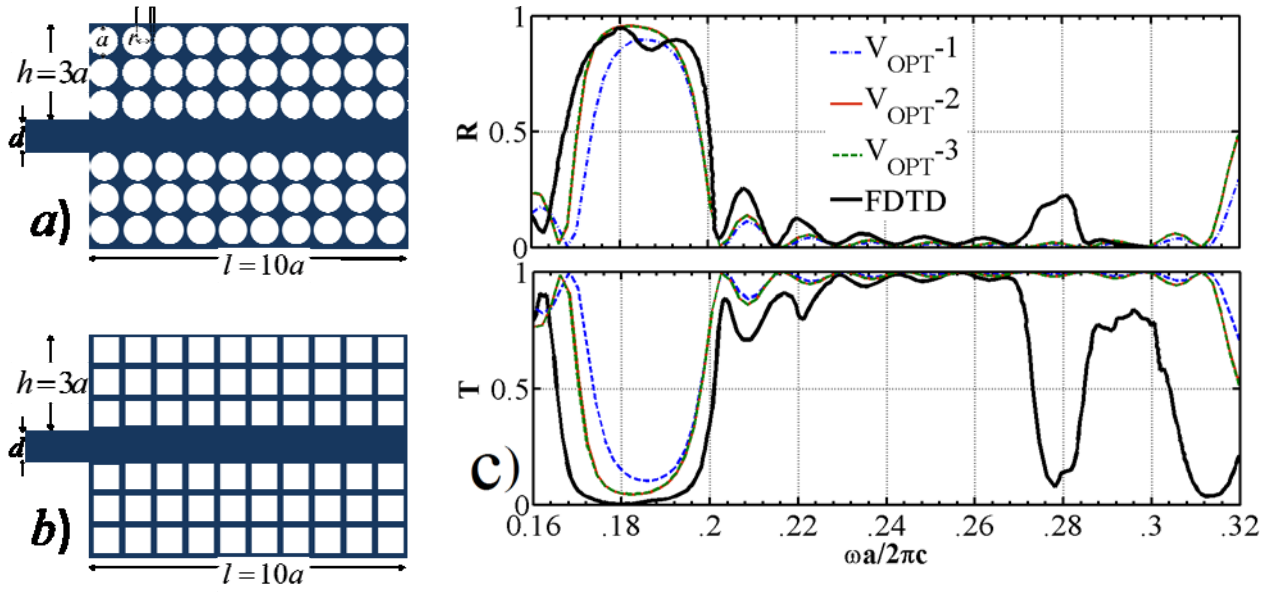

Fig 1: a) Schematic of a 2D PBG waveguide, b) Schematic of structure modified to apply V_{OPT} method. c) Reflection and transmission characteristics for V_{OPT} iterations and FDTD results [3].

References

[1] P. Bindal, A. Sharma, *Opt. Quantum. Electron.* **42**, 435 (2011). Also in *OWTNM 2010*.
[2] A. Sharma, P. Bindal, *Opt. Quantum. Electron.* **24**, 1359 (1992); A. Sharma, *ibid* **21**, 517 (1989).
[3] Ali Adibi *et al*., J. Lightwave Technol., **18**, 1554 (2000).

Fourier Series Based 3D Bi-directional Propagation Algorithm for Integrated Photonics

Jiří Čtyroký
Department of Guided-Wave Photonics
Institute of Photonics and Electronics AS CR, v.v.i.
Prague 8, Czech Republic
ctyroky@ufe.cz

Pavel Kwiecien and Ivan Richter
Department of Physical Electronics,
Faculty of Nuclear Sciences and Physical Engineering
Czech Technical University in Prague, Czech Republic
pavel.kwiecien@fjfi.cvut.cz, ivan.richter@fjfi.cvut.cz

***Abstract* — A 3D bi-directional mode expansion propagation algorithm based on Fourier series using trigonometric functions is briefly described. Nonlinear complex coordinate transformations are used as boundary conditions in transversal coordinates. In vertical direction, the adaptive spatial resolution algorithm can be alternatively applied, too. Mirror symmetries can be fully utilized to reduce numerical effort. Applications to a subwavelength-grating waveguide SOI mode transformer and a novel planar metal-dielectric slot waveguide are shown.**

Keywords-numerical modeling; bi-directional mode expansion; Fourier modal methods; plasmonic slot waveguide; subwavelength-grating waveguide

I. INTRODUCTION

Numerical modelling is an ever more important part of analysis and design of novel integrated photonic structures and devices. Despite the tremendous progress in computing power and memory of modern computers, realistic 3D modelling still remains rather challenging. Perhaps the most frequently used method for modelling 3D structures is the well-known finite-difference time domain (FDTD) method. Modelling of structures larger than just a few wavelengths in each direction is, however, still rather demanding. Frequency-domain modal methods are generally less flexible but bring deeper physical insight into the wave effects in photonic structures, and are especially well suited for modelling structures consisting of longitudinally uniform segments. In this contribution, a fully vectorial 3D bi-directional mode expansion propagation algorithm based on trigonometric Fourier series is presented. It represents an extension of a 2D method [1] into 3D. Similar as in [1], nonlinear complex coordination transformations [2] are used in both transversal coordinates as efficient perfectly matched layers (PML). The application of trigonometric (sin and cos) expansion functions instead of complex exponentials typically used in Fourier modal methods enables to fully utilize mirror symmetries of the problem to reduce the problem size without any additional effort. It is known that adaptive spatial resolution algorithm (ASR) [3, 4] helps significantly reduce the numerical effort, but it makes modelling of complex devices difficult. For this reason it can be alternatively applied only to one – vertical – direction. Fourier factorization rules [4,5] are correctly applied in both transversal directions using the approach described in [6]. The full-vector mode solver is based on transversal components of magnetic field intensity.

II. THE ALGORITHM

The structure to be modelled is considered as a concatenation of a finite number of longitudinally uniform sections. In each section, the piecewise-constant transversal permitivity distribution is supposed. Infinite transversal cross-section of a real structure is mapped into a finite calculation window (shown in Fig. 1) using nonlinear complex coordination transformations $x \rightarrow x'$, $y \rightarrow y'$ described in [2]. Coloured (shadowed) part of the cross-section represents the transformed (PML) region, the white central part of the cross-section is not modified by the transformation.

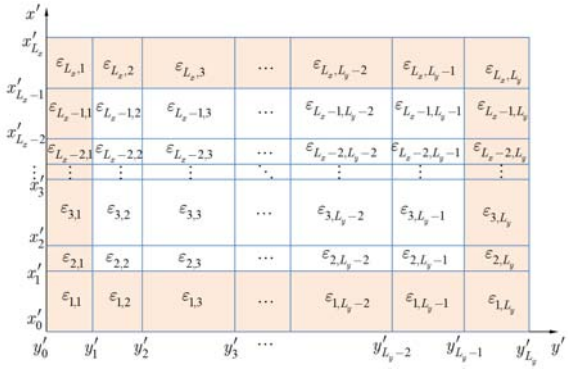

Figure 1. Transversal computation window with schematic representation of a piecewise-constant permittivity distribution after the complex nonlinear transformation.

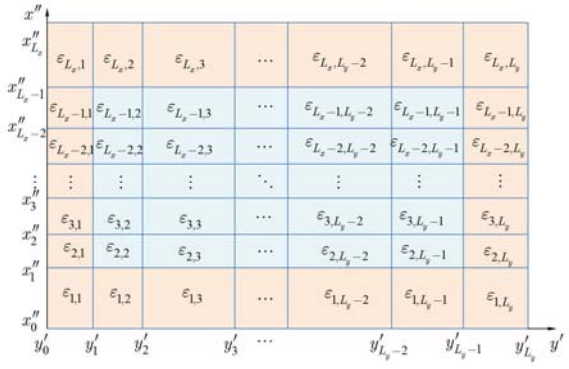

Figure 2. Transversal computation window after the application of the ASR transformation in vertical (x) direction.

Another transformation – the ASR transformation [3, 4] – can be alternatively applied to the vertical (x) coordinate at the inner part of the cross-section. After the transformation, the thicknesses of all inner horizontal layers become identical (see Fig. 2), the transformed vertical permittivity distribution becomes almost smooth, and thus the number of Fourier expansion terms required for sufficient accuracy is significantly reduced. This algorithm is thus well suited not only for modelling integrated photonic components fabricated by 2D patterning of a layered planar structure as SOI, InP, silica-on-silicon and similar devices, but also for 3D structures with metallic (plasmonic) components.

III. EXAMPLES

As a convergence test of the basic algorithm, the effective refractive index of the quasi-TE_{00} mode of a silicon nanowire embedded in SiO_2 versus the number of expansion terms is shown in Fig. 1. The results of the film mode matching method [10] were used as a reference.

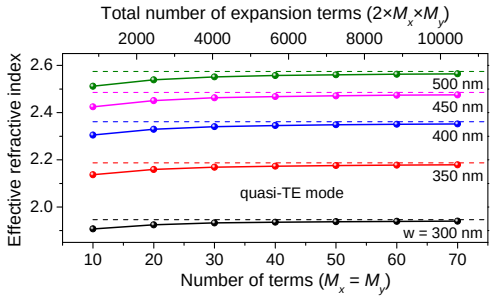

Figure 3. Effective refractive index of the fundamental quasi-TE mode of a silicon nanowire embedded in SiO_2 versus the number of Fourier expansion terms. The wire height is 260 nm, the width varies from 300 to 500 nm. The wavelength is 1550 nm.

As a next example, calculated optical field distribution in the SOI subwavelength grating waveguide mode transformer [8] embedded in SU8 resist with 60 subwavelength sections is shown in Fig. 4. The calculated coupling losses at the wavelength of 1550 nm are 0.61 dB and 0.45 dB for TE_{00} and TM_{00} mode, respectively. 60×70 Fourier terms were used in the calculation.

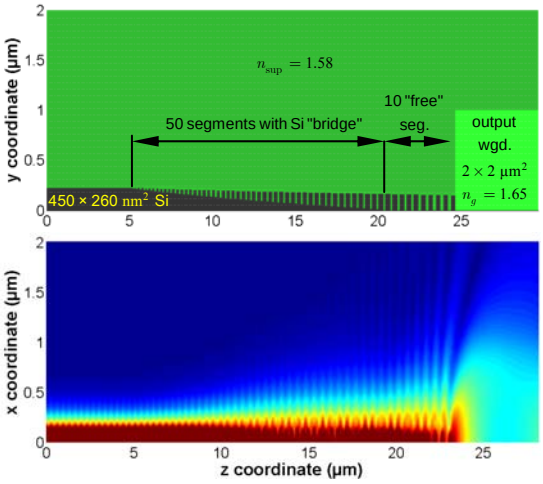

Figure 4. a) Top view of the mode transformer; because of symmetry, only one half of the structure is considered.
b) calculated optical field distribution, TE_{00} excitation. Perfectly conducting magnetic wall was placed at the symmetry plane.

In Fig. 5, the cross-section and the calculated mode field distribution of a metal-dielectric slot waveguide [9] is plotted. The waveguide is formed by a very thin Si nanowire embedded in SiO_2 and separated from an Au layer by a 30 nm slot. 80×60 Fourier terms were used. Fig. 6 shows the geometry and the field distribution of a very sharp S-bend in this waveguide. All these results have been, in fact, checked with another our modal method, namely aperiodic rigorous coupled wave analysis (aRCWA) technique, their comparison will be shown.

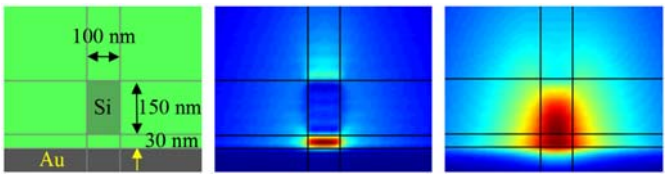

Figure 5. a) Cross-section of the metal-dielectric slot waveguide, b) vertical electric field component, c) horizontal magnetic field component of the plasmonic mode.

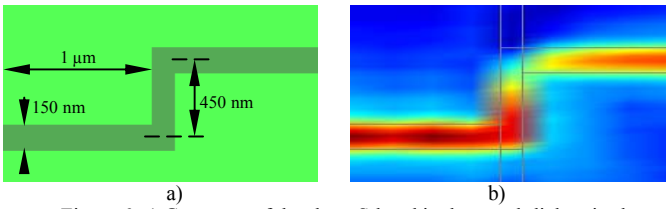

Figure 6. a) Geometry of the sharp S-bend in the metal-dielectric slot waveguide, b) distribution of a vertical electric field component.

IV. ACKNOWLEDGMENTS

This work was financially supported by the Czech Science Foundation and the Ministry of Education, Youth and Sports of the Czech Republic (projects P205/10/0046, P205/12/G118, OC09061 and OC09038).

[1] J. Čtyroký, "Improved bidirectional-mode expansion propagation algorithm based on Fourier series," J. Lightwave Technol., Vol. 25, pp. 2321-2330, 2007.

[2] J. P. Hugonin and P. Lalanne, "Perfectly matched layers as nonlinear coordinate transforms: a generalized formalization," J. Opt. Soc. Amer. A, Vol. 22, pp. 1844-1849, 2005.

[3] T. Vallius and M. Honkanen, "Reformulation of the Fourier modal method with adaptive spatial resolution: application to multilevel profiles," Optics Express, Vol. 10, pp. 24-34, 2002.

[4] J. Čtyroký, P. Kwiecien, and I. Richter, "Fourier Series-Based Bidirectional Propagation Algorithm with Adaptive Spatial Resolution," J. Lightwave Technol. Vol. 28, pp. 2969-2976, 2010.

[5] P. Lalanne and G. M. Morris, "Highly improved convergence of the coupled-wave method for TM polarization," J. Opt. Soc. Amer. A, Vol. 13, pp. 779-784, 1996.

[6] L. Li, "Use of Fourier series in the analysis of discontinuous periodic structures," J. Opt. Soc. Amer. A, Vol. 13, pp. 1870-1876, 1996.

[7] L. Li, "Fourier modal method for crossed anisotropic gratings with arbitrary permittivity and permeability tensors," J. of Optics A: Pure and Applied Optics, Vol. 5, pp. 345-355, 2003.

[8] P. Cheben, P. J. Bock, J. H. Schmid, et al., "Refractive index engineering with subwavelength gratings for efficient microphotonic couplers and planar waveguide multiplexers," Optics Letters, vol. 35, pp. 2526-2528, 2010.

[9] M. Fujii, J. Leuthold, and W. Freude, "Dispersion Relation and Loss of Subwavelength Confined Mode of Metal-Dielectric-Gap Optical Waveguides," IEEE Phot. Technol. Letters, vol. 21, pp. 362-364, 2009.

[10] L. Prkna, M. Hubálek, and J. Čtyroký, "Field modeling of circular microresonators by film mode matching," IEEE Journal of Selected Topics in Quantum Electronics, vol. 11, pp. 217-223, 2005.

Optical waveguide engineering for demanding applications

I. Molina-Fernández, Robert Halir, A. Ortega-Moñux, L. Zavargo-Peche, S. Romero-Garcia, D. Pérez-Galacho, J. G. Wangüemert-Pérez
Departamento de Ingeniería de Comunicaciones
Universidad de Málaga, UMA
Málaga, Spain
imf@ic.uma.es

Pavel Cheben, Dan-Xia Xu
Institute for Microstructural Sciences
National Research Council, NRC
Ottawa, Canada

***Abstract*—New demanding applications, such as 100Gb Ethernet WDM systems and high speed optical interconnects, require high performance photonic components. Sub-wavelength gratings (SWG) enable refractive index engineering in silicon waveguides, and open new design strategies which can be advantageously used for component improvement. In this work, we will show several SWG waveguide devices which exhibit improved performance.**

Keywords; Subwavelength gratings, silicon-on-insulator, SWG, photonic components

I. INTRODUCTION

Silicon-on-Insulator (SoI) is emerging as a major fabrication platform for integrated optics, owing to its high contrast that enables compact and highly integrated devices, and its compatibility with CMOS fabrication processes. Recently a new type of silicon waveguide, the Sub-Wavelength Grating (SWG), was presented and experimentally shown to exhibit low losses [1]. SWG consists of waveguide segments which are arrayed periodically with a pitch that is small enough to frustrate diffraction, i.e.

$$\Lambda < \Lambda_{Bragg} = \lambda / (2 \cdot n) \qquad (1)$$

In the subwavelength regime the waveguide behaves as having an effective refractive index and birefringence that can be engineered by changing the duty cycle and/or pitch of the SWG structure. Applications of SWG have been demonstrated in several devices of practical interest as, for example, efficient fiber-to-chip couplers [2], waveguide crossings [3], arrayed waveguide gratings [4] and high performance MMIs [5]. In this paper we will describe novel design approaches for several important devices in SoI. It will be shown that, depending on the specific application SWG structures can be engineered to tailor the required value of the refractive index, the chromatic dispersion and/or the birefringence of the equivalent material.

II. FIBER TO CHIP GRATING COUPLER

Light coupling from optical fibers to Silicon Wires (SW) is challenging due to the large size mismatch between the fiber and the waveguide. Grating couplers are an interesting alternative for this function. Efficient grating couplers require the radiated field to be matched with the fiber mode, which, in turn, is achieved by adjusting the amount of power extracted from the grating per unit length. This is usually achieved by using a shallow etch to define the grating [6] but this solution requires a two etch step solution. Alternatively, using SWGs to define the grating, as shown in Fig. 1(a), allows for fabrication of the structure in the same full etch step as the waveguides, thereby simplifying fabrication. Fig. 1(b) shows a SEM image of a uniform grating coupler fabricated with 193nm DUV lithography at LETI which allows mass fabrication. The fabricated couplers exhibited a coupling efficiency of -5dB and a 55 nm 3dB bandwidth in the C band

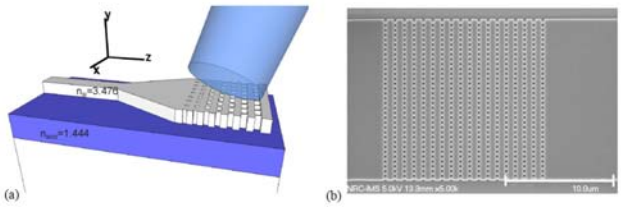

$$\alpha + \beta = \chi. \qquad (1) \qquad (1)$$

Figure 1. Single etch SW SWG grating coupler (a) Concept. (b) SEM image of fabricated coupler

III. MULTIMODE INTERFERENCE COUPLERS

The same type of approach can be used to design high performance MMI couplers as those required for advanced coherent receivers that are being developed for 100Gb/s Ethernet and beyond [7]. It is well known that reducing the index contrast in SW MMIs can redound in significant performance improvement [8] but at the expense of higher cost and complexity. This can be seen in Fig. 2(a) where modal phase errors in a SoI fully etched 2x4 MMI (square-dashed curve) is compared with a shallow etched situation (circle-dashed curve). Alternatively, we propose the use of SWGs to

emulate this effect. As shown in Fig. 2(a), arraying the SWG in the x-direction does not yield a significant enhancement (square-solid curve), but arraying the SWG along the z-direction yields the desired effect, effectively reducing the phase error for most of the MMIs modes (circle-solid curve). As shown in Fig. 2(b) the SWG based design significantly enhances the performance of the 2x4 MMI.

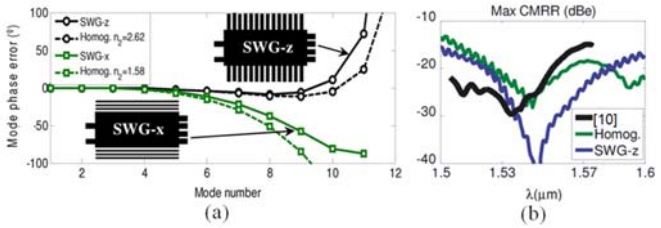

Figure 2. (a) Modal phase error in a 2x4 MMI (b) Simulated common mode rejection ratio

IV. Polarization Splitter

It is well known that SW MMIs can be used as polarization splitters by exploiting the different phase velocities that TE and TM modes suffer in the MMI core. However, due to the relatively small birefringence value of SW, this technique yields long devices. SWG structures can be used to increment the underlying birefringence of the MMI core and reduce its size. In doing so we have designed a SWG MMI compact polarization splitter that exhibits an eightfold length reduction and +5dB improvement in splitting ratio as compared with previous MMI based splitters.

V. Taper Optimization

The use of SWGs in device design will require low loss transitions between different SWG structures. In homogeneous waveguides low loss tapers can be achieved with a sufficiently long linear taper between the two waveguides. However this is not always the case when dealing with SWG based devices.

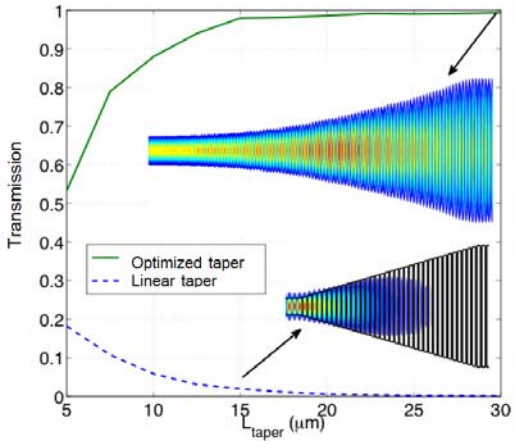

Figure 3. Simulated transmission through a linear (lower) and optimized (upper) taper between two SWG waveguides

Consider the SWG waveguide in the lower inset of Fig. 3 where the width and duty cycle are tapered linearly. As the length of the taper is increased, transmission decreases, and, for a length of about 25μm, the taper acts like a virtually perfect reflector. While neither the initial (narrow) waveguide nor the final (wide) waveguide are in the Bragg regime, some of the intermediate periods are in the Bragg regime, which produces the undesired back reflection. Tapers thus have to be designed carefully, to avoid these zones. In the particular example considered here, choosing a quadratic width variation avoids the Bragg regime along the taper (see upper inset in Fig. 3), and transmission through the taper approaches unity as the taper length is increased.

VI. Conclusions

SWG structures offer new design possibilities arising from the fact that refractive index, chromatic dispersion, or birefringence can be optimized by SWG parameters engineering. These concepts can be directly applied in the SoI platform, because the required small feature sizes (generally below 200nm) can readily be fabricated not only with research oriented e-beam lithography but also in using large-scale deep ultraviolet lithography.

Acknowledgments

This work was supported by the Spanish Ministerio de Ciencia (project TEC2009-10152), the Andalusian Regional Ministry of Science, Innovation and Business (project P07-TIC-02946), and the European Mirthe project (FP7-2010-257980).

References

[1] P. Cheben, D.-X. Xu, S. Janz, A. Densmore, “Subwavelength waveguide grating for mode conversion and light coupling in integrated optics”, Opt. Express, vol. 14, pp. 4695–4702, May 2006.

[2] R. Halir, L. Zavargo-Peche, D.-X. Xu, P. Cheben, R. Ma, J. H. Schmid,S. Janz, A. Densmore, A. Ortega-Moñux, Í. Molina-Fernández, M. Fournier, J.-M. Fédeli, “Single etch grating couplers for mass fabrication with DUV lithography”, Opt. Quant. Electron., Accepted.

[3] P. J. Bock, P. Cheben, J. H. Schmid, J. Lapointe, A. Delâge, D.-X. Xu, S. Janz, A. Densmore, T. J. Hall, “Subwavelength grating crossing for silicon wire waveguides”, Opt. Express, vol. 18, pp. 16146–16155, July 2010.

[4] P. Cheben, P. J. Bock, J. H. Schmid, J. Lapointe, S. Janz, D.-X. Xu, A. Densmore, A. Delâge, B. Lamontagne, T. J. Hall, “Refractive index engineering with subwavelength gratings for efficient microphotonic couplers and planar waveguide multiplexers”, Opt. Lett., vol. 35, pp. 2526–2528, August 2010.

[5] A. Ortega-Moñux, L. Zavargo-Peche, A. Maese-Novo, Í. Molina-Fernández, R. Halir, J. G. Wangüemert-Pérez, P. Cheben, J. H. Schmid, “High-performance multimode interference coupler in silicon waveguides with subwavelength structures”, IEEE Photon. Technol. Lett., vol. 23, pp. 1406–1408, October 2011.

[6] Tang Y., Wang Z., Wosinski L., Westergren U., He S. “Highly efficient nonuniform grating coupler for silicon-on-insulator nanophotonic circuits”, Opt. Lett. 35, 1290-1292 (2010)

[7] http://www.ist-mirthe.eu/

[8] Halir R., Roelkens G., Ortega-Moñux A., and Wangüemert-Pérez J. G., “High-performance 90 hybrid based on a silicon-on-insulator multimode interference coupler,” Opt. Lett. 36, 178–180 (2011)